



Finger Print History, Registration, Enhancement, and Minutias Detection

Daniel Novák

3.10. 2019, Prague

**Acknowledgments: Xavier Palathingal, Andrzej Drygajlo,
Handbook of Fingerprint Recognition**

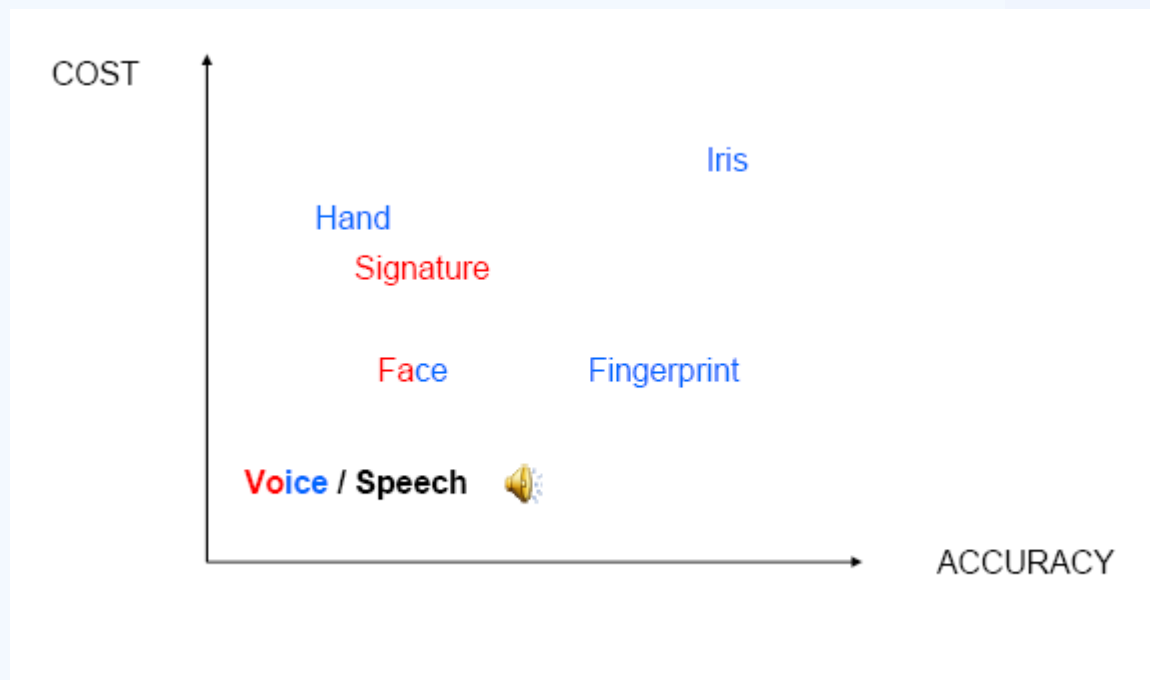


laboratory
Gerstner



Outline

- Introduction to Fingerprint
- History
- Registration
- Enhancement
- Minutiae detection



Fingerprint



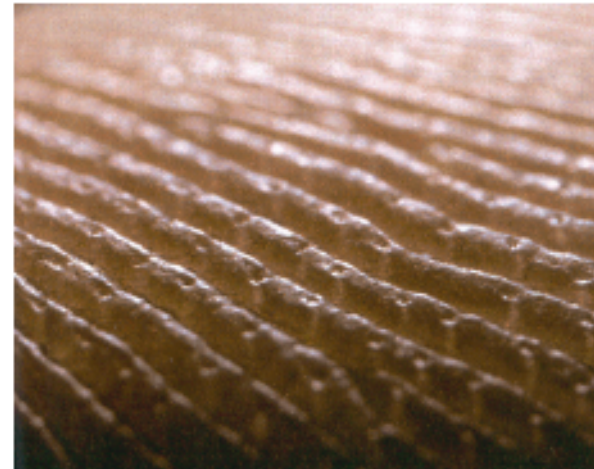
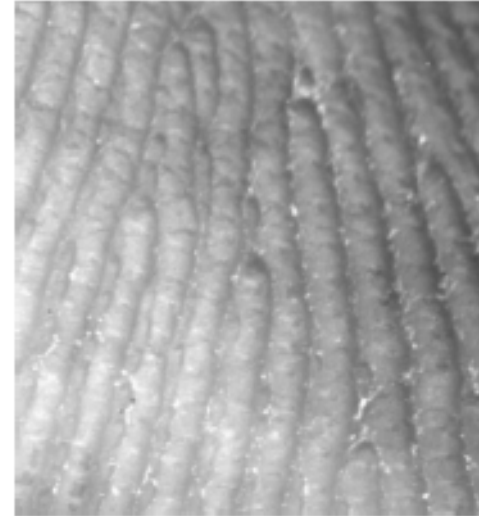
- Fingerprints are "permanent" in that they are formed in the fetal stage, prior to birth, and remain the same throughout lifetime
- The changes can be made by: flexibility from the skin, growing, a dirty finger, scarring, a wound, or a disease of the skin
- They are only weakly determined by genetics, e.g. identical (monozygotic, one egg) twins (the same DNA) have fingerprints that are quite different
- Fingerprints of an individual are "unique"; they indeed are distinctive to a person
- The right definition of a fingerprint is strictly speaking the **print (stamp)** that a finger left on an object



Fingerprint



- The inside surfaces of hands and feet of humans (and, in fact, all primates) contain minute ridges of skin with furrows between each ridge
- The purpose of this skin structure is to:
 - Facilitate exudation of perspiration
 - Enhance sense of touch
 - Providing a gripping surface



No fingerprint?



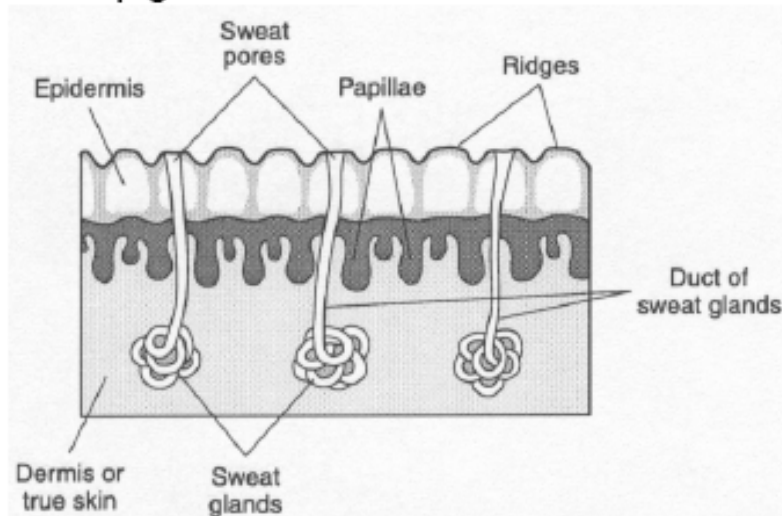
- In very rare cases there are people that do not have prints. Not on their fingers, their palms or their feet. They were born with it or the friction ridges have degenerated during their lives
- Approximately **4%** of fingerprint images have been observed to have poor ridge details



Friction Skin



- **Friction skin** differs significantly in structure and function from the skin covering the rest of the body:
 - It is hairless
 - It contains no sebaceous (oil) glands
 - It has a much higher concentration of nerve endings
 - It has a much higher concentration of sweat glands
 - There is a lack of pigmentation



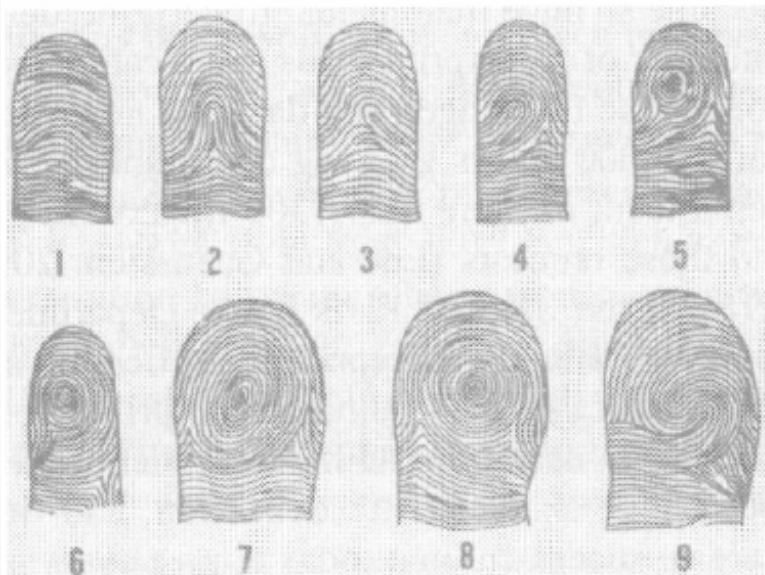
History of fingerprints



- Human fingerprints have been discovered on a large number of archaeological artifacts and historical items
- In 1684, the English plant morphologist, [Nehemiah Grew](#), published the first scientific paper reporting his systematic study on the ridge, furrow, and pore structure
- In 1788, a detailed description of the anatomical formations of fingerprints was made by [Mayer](#).
- In 1823, [Purkinji](#) proposed the first fingerprint classification, which classified into nine categories
- [Sir Francis Galton](#) introduced the minutae features for fingerprint matching in late 19th century
- 1924, an act of U.S. Congress established the Identification Division of the FBI (Federal Bureau of Investigation) with a database of 810 000 fingerprint cards.
TODAY: 200 mil !!!



Purkynje classification & Galton individuality & FBI



MR. FRANCIS GALTON'S ANTHROPOMETRIC LABORATORY.

The Laboratory communicates with the "Western Gallery" in which the Scientific Collections of the South Kensington Museum are contained. The Western Gallery runs parallel to Queen's Gate, and is entered either from Queen's Gate or from the new Imperial Institute Road. The latter entrance is close to the Laboratory. Admission is free.

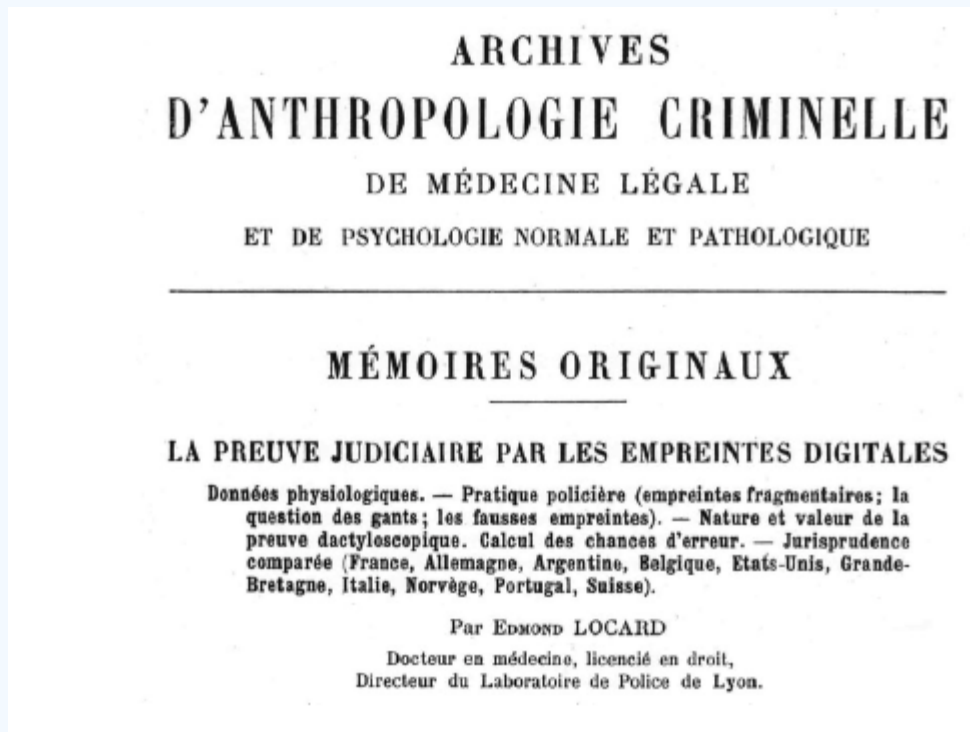
Date of Measurement.			Initials.	Birth-day.			Eye Color.	Sex.	Single, Married, or Widowed?	Page of Register.	
Day.	Month.	Year.		Day.	Month.	Year.					
20	12	89	J. H. S.	22	2	70	Brown Grey	m	S	2310	
Head length, maximum	Head breadth, maximum	Height standing, less heels of shoes.	Span of arms from opposite finger tips.	Weight in ordinary clothing.	Strength of grasp. Right hand.	Left hand.	Breathing capacity.		Distance of reading diamond instrument. Right eye.	Snellen's type read at 20 feet. Left eye.	Color Sense.
Inch. Tenths.	Inch. Tenths.	Inch. Tenths.	Inch. Tenths.	In. Do.	Do.	Do.	Cubic inches.	Inches.	Inches.	No. of Type	? Normal.
7.3	5 9/2	66.6	67	7 128	93	88	200	19	19.	56	Yes
Height sitting above seat of chair.	Height of eye of knee, when sitting, less heels.	Length, elbow to finger tip, left arm.	Length of middle finger of left hand.	Knowledge of hearing.	Height audible tone. (By whistle)	Reaction time.		Left Thumb.		Right Thumb.	
Inch. Tenths.	Inch. Tenths.	Inch. Tenths.	Inch. Tenths.	? Normal.	Vibrations per second.	Headwidths of a second.	To sight.	To sound.			
65.5	20 7	17.7 1/2	4 5	Yes	21,000	15	15				

One page of the Register is assigned to each person measured, in which his measurements at successive periods are entered in successive lines. No names appear on the Register. Copies of the entries can be obtained through application of the persons measured, or by their representatives, under such conditions and restrictions as may be fixed from time to time.

Fingerprints as evidence



- 1892–Juan Vucetich(Argentina) made the first criminal fingerprint identification
- 1914 –Edmond Locard wrote that if 12 points(Galton’s details) were the same between two fingerprints, it would suffice as a positive identification.



History of fingerprints

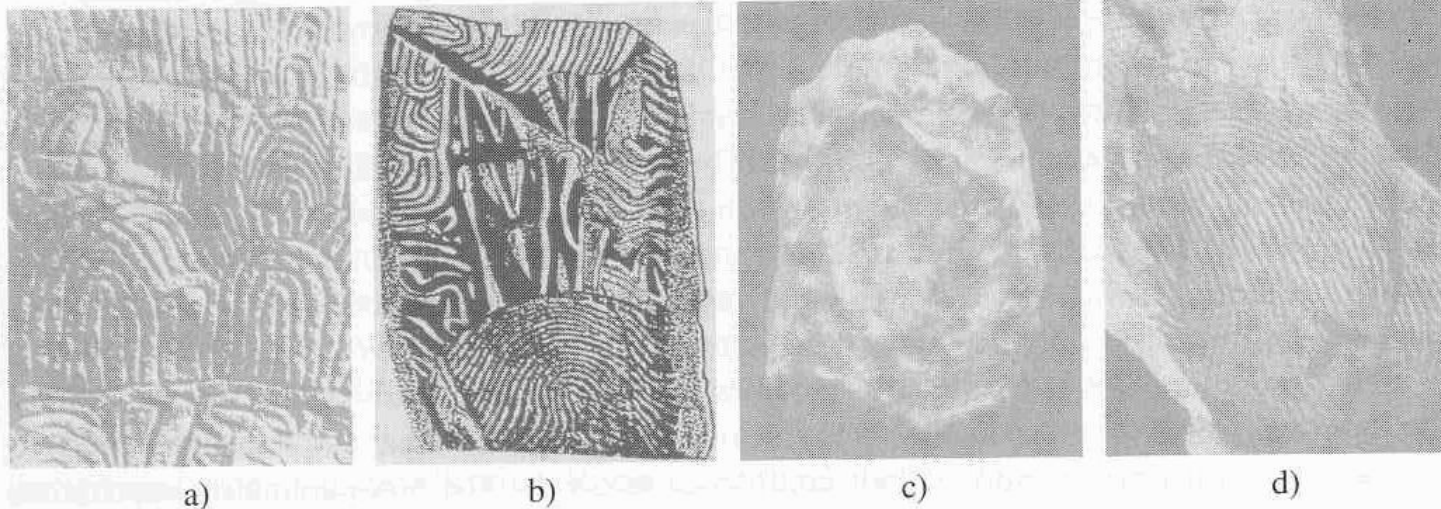


Figure 1.8. Examples of archaeological fingerprint carvings and historic fingerprint impressions
a) Neolithic carvings (Gavrinis Island) (Moenssens, 1971); b) standing stone (Goat Island, 2000 B.C.) (Lee and Gaensslen, 2001); c) a Chinese clay seal (300 B.C.) (Lee and Gaensslen 2001); d) an impression on a Palestinian lamp (400 A.D.) (Moenssens, 1971). Although impressions on the Neolithic carvings and the Goat Island standing stones might not be used to indicate identity, there is sufficient evidence to suggest that the Chinese clay seal and impressions on the Palestinian lamp were used to indicate the identity of the providers. Figures courtesy of A. Moenssens, R. Gaensslen, and J. Berry.



Formation of fingerprints



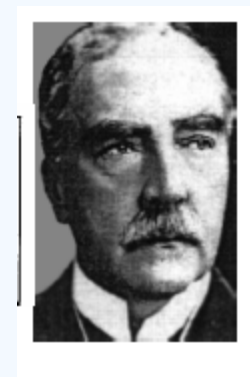
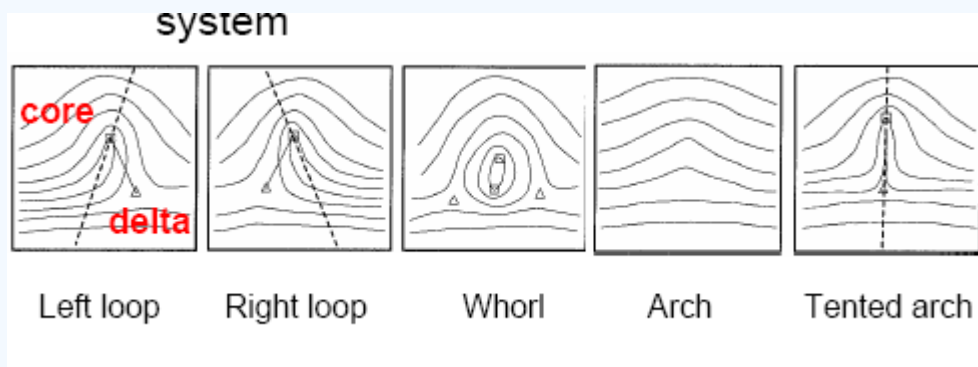
- Fingerprints are fully formed at about **seven months** of fetus development
- General characteristics of the fingerprint emerge as the skin on the fingertip begins to differentiate.
- flow of amniotic fluids around the fetus and its position in the uterus change during the differentiation process
- Thus the cells on the fingertip grow in a microenvironment that is slightly different from hand to hand and finger to finger



Fingerprint feature extraction



- Fingerprint pattern, when analyzed at different scales, exhibits different types of features
 - global level - delineates a ridge line flow pattern
 - » Sir Edward Henry 1897
 - local level – minute details can be identified
 - Very fine level – intra-ridge details can be detected



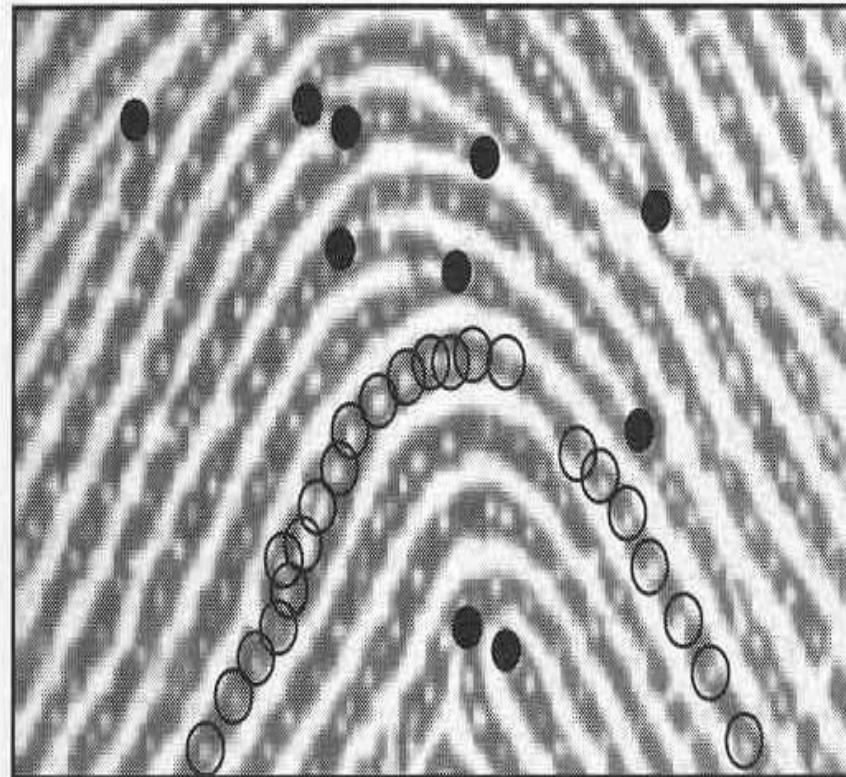


Figure 1.13. Minutiae (black-filled circles) in a portion of fingerprint image; sweat pores (empty circles) on a single ridge line.

Difficulty in fingerprint matching



- Fingerprint matching is a difficult problem due to large variability in different impressions of the same finger
- Main factors responsible for intra-class variations are: displacement, rotation, partial overlap, non-linear distortion, variable pressure, skin condition, noise and feature extraction errors



Two impressions
from the same finger



Two impressions
from different fingers



Fingerprint classification and Indexing



- To reduce the search time and computational complexity
- technique used to assign a fingerprint to one of the several pre-specified types
- Only a limited number of categories have been identified, and there are many ambiguous fingerprints

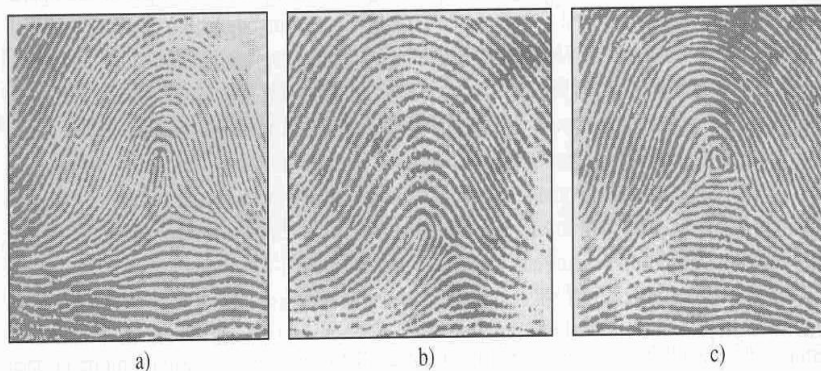


Figure 1.15. Examples of fingerprints that are difficult to classify; a) tented arch; b) a loop; c) a whorl; it seems that all the fingerprints shown here should be in the loop category.



Synthetic fingerprints



- Performance evaluation of fingerprint recognition systems is very data dependent
- To obtain tight confidence intervals at very low error rates, **large databases** of images are required and its expensive
- To solve this problem synthetic fingerprint images are introduced, **cost reduction**



The main parameters characterizing a fingerprint image are



Resolution ,Area,Number of pixels, Dynamic Range, Geometric Accuracy, Image Quality



Figure 2.15. The fingerprint on the left, acquired at 500 dpi, is compared with lower resolutions: 400, 300, and 250 dpi, respectively.

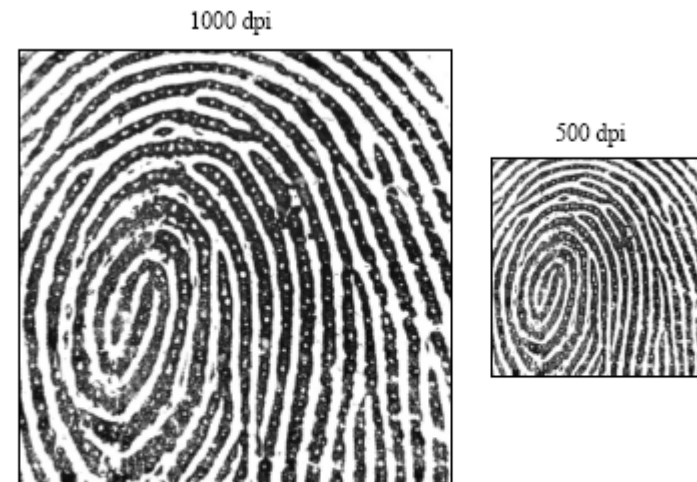


Figure 2.16. The fingerprint portion on the left is acquired at 1000 dpi; sweat pores and other fine details are clearly visible; on the right, the fingerprint portion is sub-sampled at 500 dpi while the fine details are not as clear.

Fingerprint images



Optical scanner



Capacitive scanner



Piezoelectric scanner



Thermal scanner



Inked impression



Latent fingerprint



Off-line & On-line fingerprint Acquisition



- Although the first fingerprint scanners were introduced more than 30 years ago, still ink-technique is used in some applications

Why & What are the advantages?

Because it has the possibility of producing

Rolled impressions

<http://crime.about.com/od/police/ss/fingerprints.htm>

Latent impressions

- The most important part of a fingerprint scanner is the sensor.
- All the existing scanners belong to one of the 3 families

Optical sensors

Solid state sensors

Ultrasound sensors



Rolled & Plain FP



Figure 2.3. The same finger acquired as a plain impression (on the left) and as a rolled impression (on the right): the portion of the rolled fingerprint corresponding to the plain fingerprint is highlighted.



– Daktyloskopie (Antropometrie)

- na světě neexistují dva jedinci, kteří mají absolutně shodné obrazce papilárních linií,
- obrazce papilárních linií jsou po celý život relativně neměnné,
- obrazce papilárních linií jsou trvale neodstranitelné, pokud není odstraněna zárodečná vrstva pokožky.

–0.8% zamen, v USA az 2000 případu

–**Simon A. Cole, "More Than Zero: Accounting for Error in Latent Fingerprint Identification," *Journal of Criminal Law & Criminology*, Volume 95, Number 3 (Spring 2005), pp. 985-1078.**

- 1.Shoda otisků musí být potvrzena dalším hodnotitelem.
- 2.Hodnotitel musí být spolehlivý a prověřený expert.
- 3.Pro určení shody je potřeba velký počet identifikačních rysů.
- 4.Obhájce obžalovaného si může vyžádat dodatečné posouzení shody otisků nezávislým expertem.

–<http://socialecology.uci.edu/faculty/scole>



Rolled fingerprint Impressions

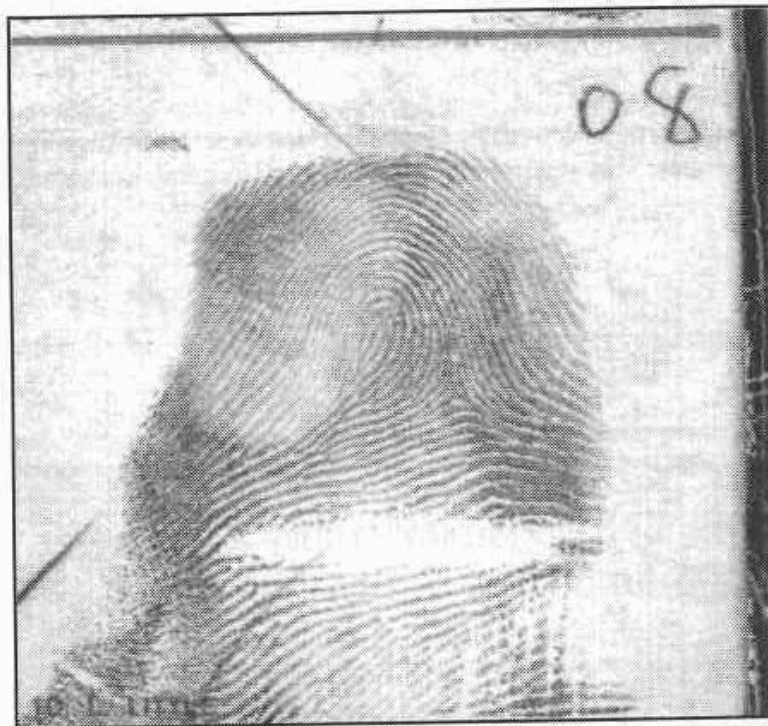


Figure 2.4. Rolled fingerprint images acquired off-line with the ink technique.



Latent fingerprint images

10 % visible

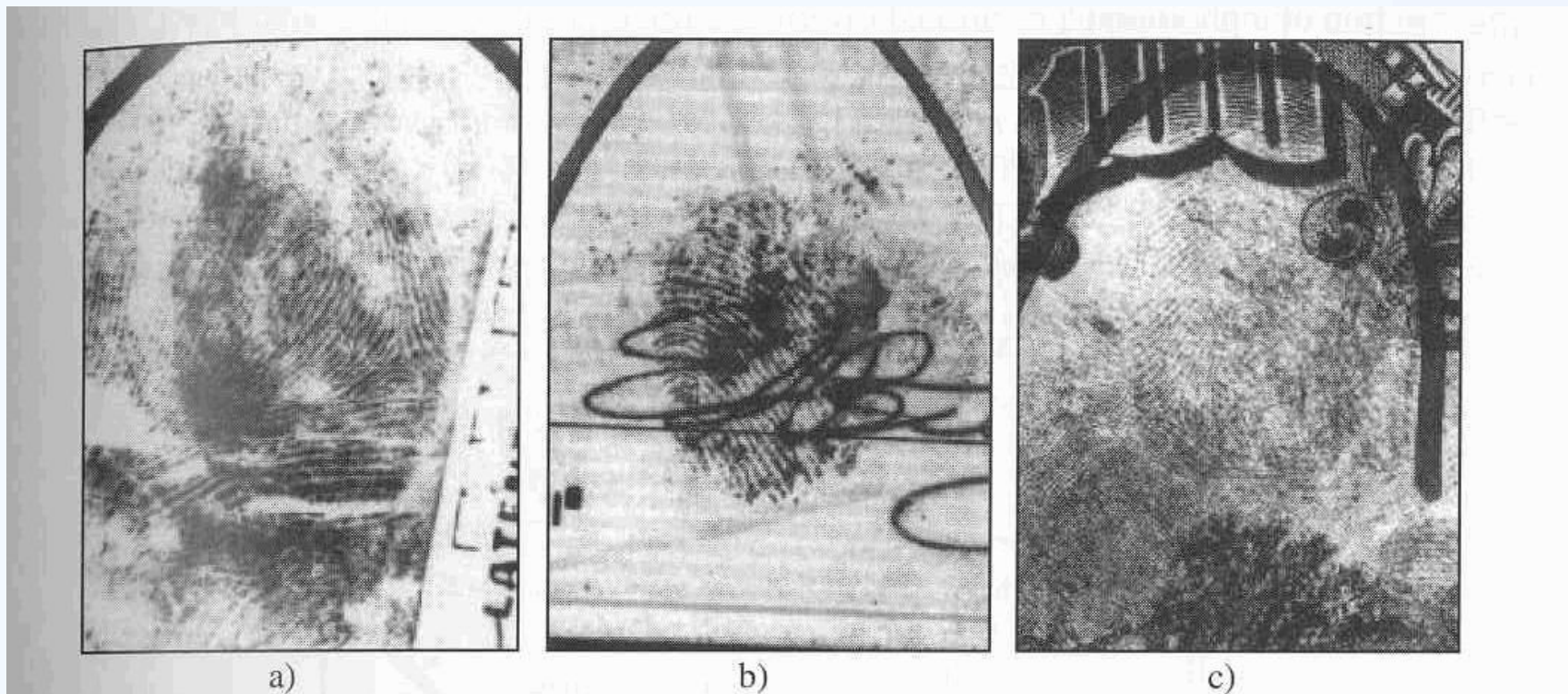


Figure 2.5. Examples of a) good, b) bad, and c) ugly latent fingerprints from NIST Special Database 27 (Garris and McCabe, 2000).



Live scan fingerprint sensing

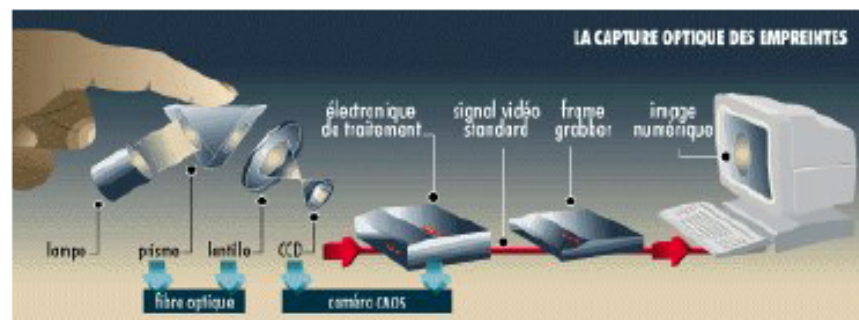
- The most important part of a fingerprint scanner is the sensor.
- All the existing scanners belong to one of the 3 families

Optical sensors

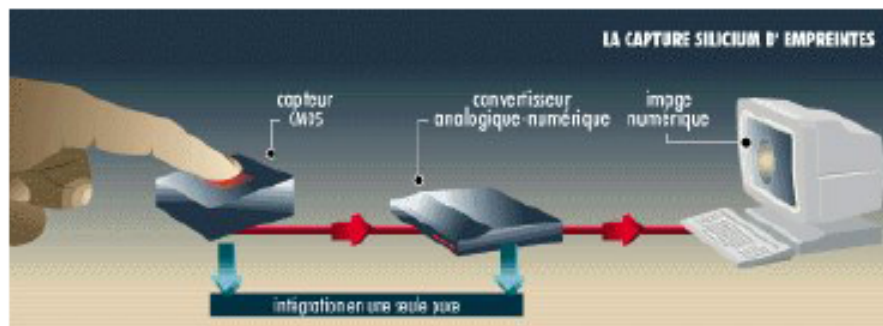
Solid state sensors

Ultrasound sensors

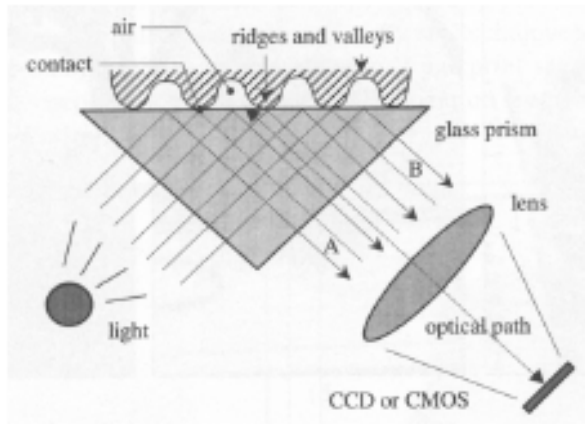
Optical scanner



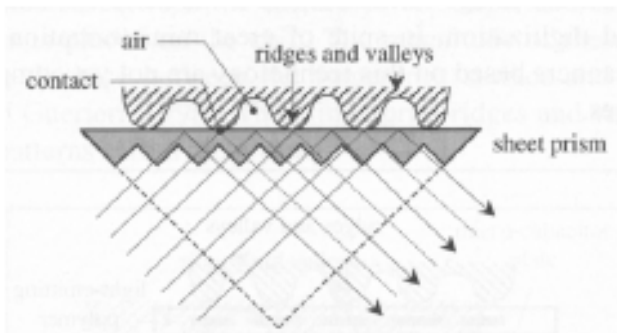
CMOS scanner



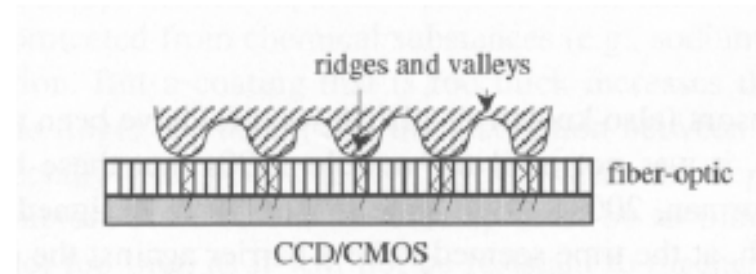
Optical sensors



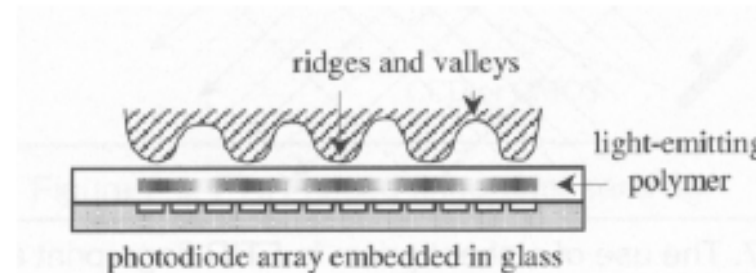
Internal reflection optical sensor



Sheet prism optical sensor



Sensor based on optical fibers



Electro-optical fingerprint sensor



Optical scanner



Good quality
fingerprint



Dry finger



Wet finger



Intrinsically
bad fingerprint

Solid state sensors



- These are designed to overcome the size and cost problems
- Silicon based sensors are used in this
- Neither optical components nor external CCD/CMOS image sensors are needed
- Four main effects have been produced to convert the physical information into electrical signals
 - Capacitive
 - Thermal
 - Electric field
 - Piezo Electric



Capacitive & Piezo- Electric

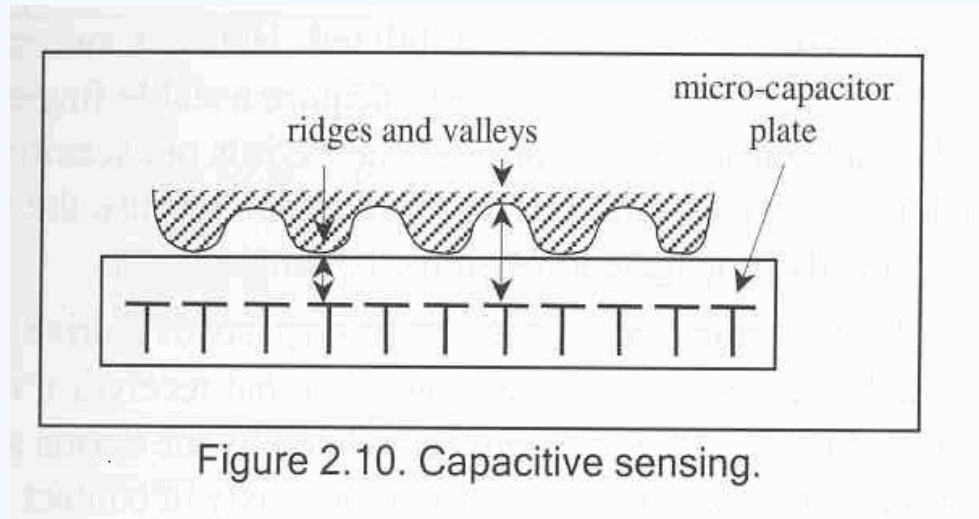


Figure 2.10. Capacitive sensing.

- Pressure sensitive sensors
- Produce an electrical signal when mechanical stress is applied to them
- Sensor surface is made up of a non-conducting dielectric material
- Ridges and valleys are present at different distances from the surface , they result in different amounts of current



Thermal sensors & Electric field



- Works based on temperature differentials
- Sensors are made of pyro electric material
- Temperature differential produces an image, but this image soon disappears
 - because the thermal equilibrium is quickly reached and pixel temperature is stabilized
- Solution is sweeping method
- Advantages
 - Not sensitive to ESD
 - Can accept thick protective coating
- **Electric field**
- Sensor consists of drive ring
- This generates a sinusoidal signal and a matrix of active antennas
- To image a fingerprint, the analogue response of each element in the sensor matrix is amplified, integrated and digitized



Ultrasound sensors



– Principle is Echography

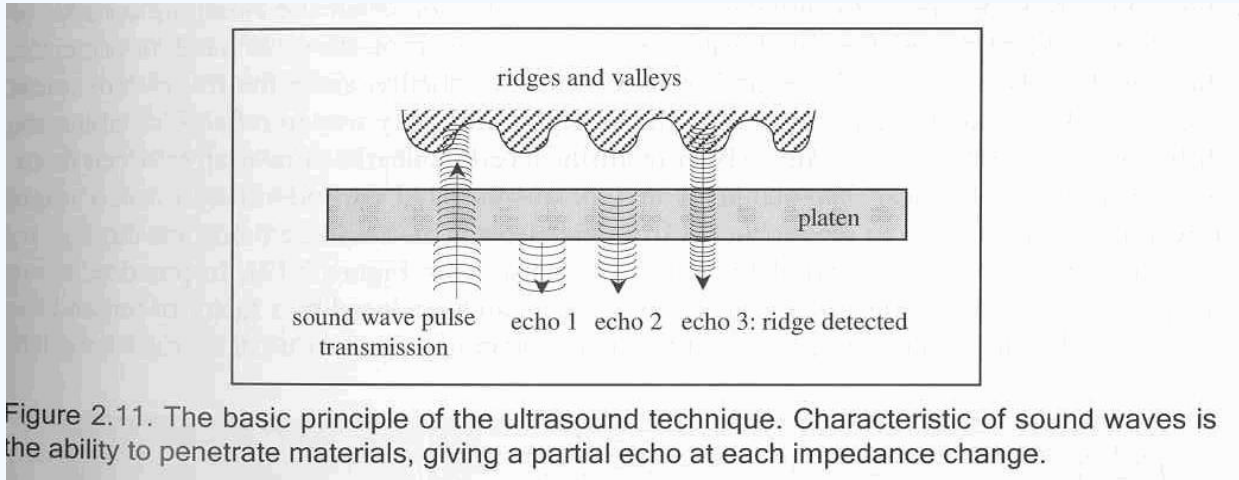


Figure 2.11. The basic principle of the ultrasound technique. Characteristic of sound waves is the ability to penetrate materials, giving a partial echo at each impedance change.

– Advantages of Ultrasound sensors

Good Quality images

– Disadvantages

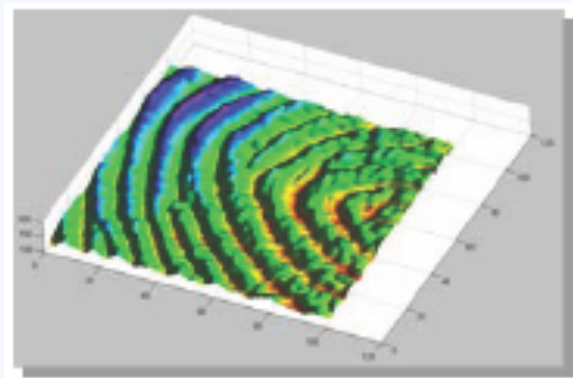
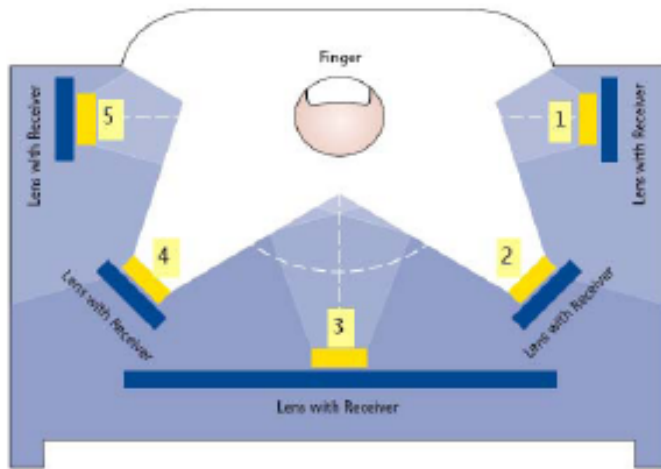
Scanner is large

Mechanical parts are quite expensive



laboratory
Gerstner

Touchless sensor: TBS – Surround Imager



3D Imaging (correct)



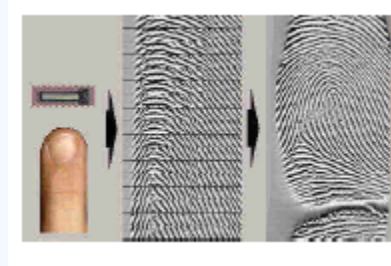
2D imaging (wrong)



Touch Vs Sweep



- Drawbacks of Touch method
 - Sensor can become dirty
 - Visible latent fingerprints remains on the sensor
 - Rotation of the fingerprint may be a problem
 - Strict trade-off between the cost and the size of the sensing area



Advantages and drawbacks of Sweeping Method

- Equilibrium is continuously broken when sweeping, as ridges and valleys touch the pixels alternately, introducing a continuous temperature change
- Sensors always look clean
- No latent fingerprints remain
- No rotation
- Novice user may encounter difficulties
- Interface must be able to capture a sufficient number of fingerprint slices
- Reconstruction of the image from the slices is time consuming

Sweeping Method

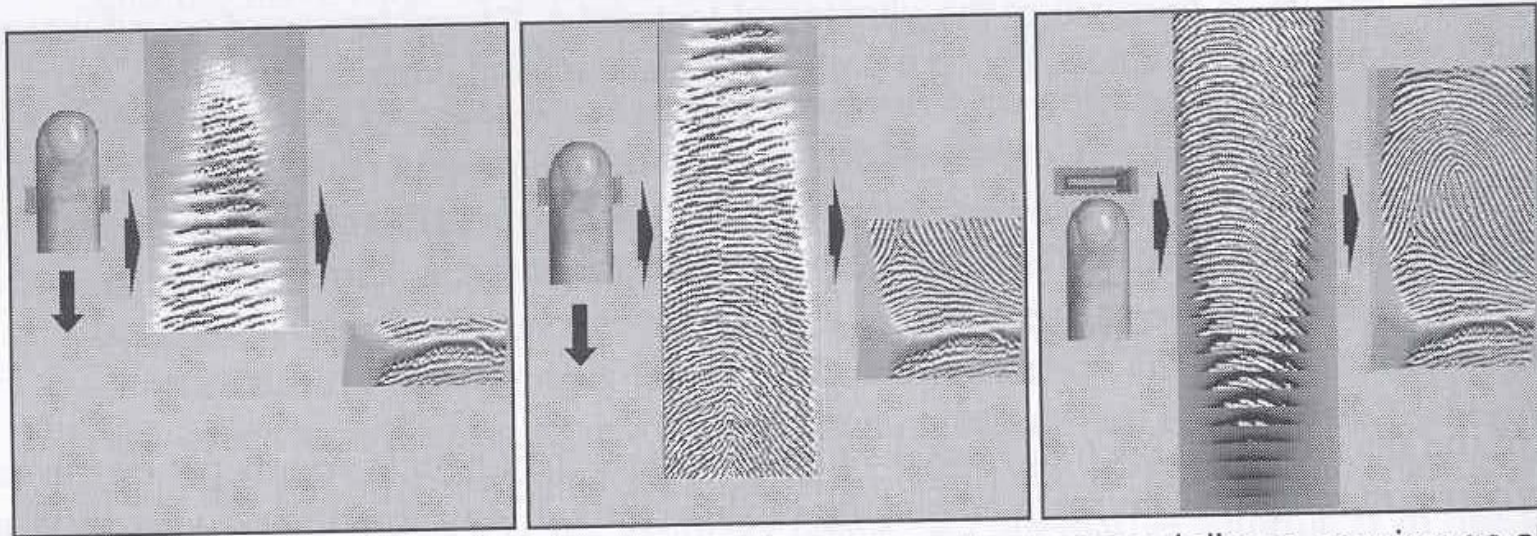
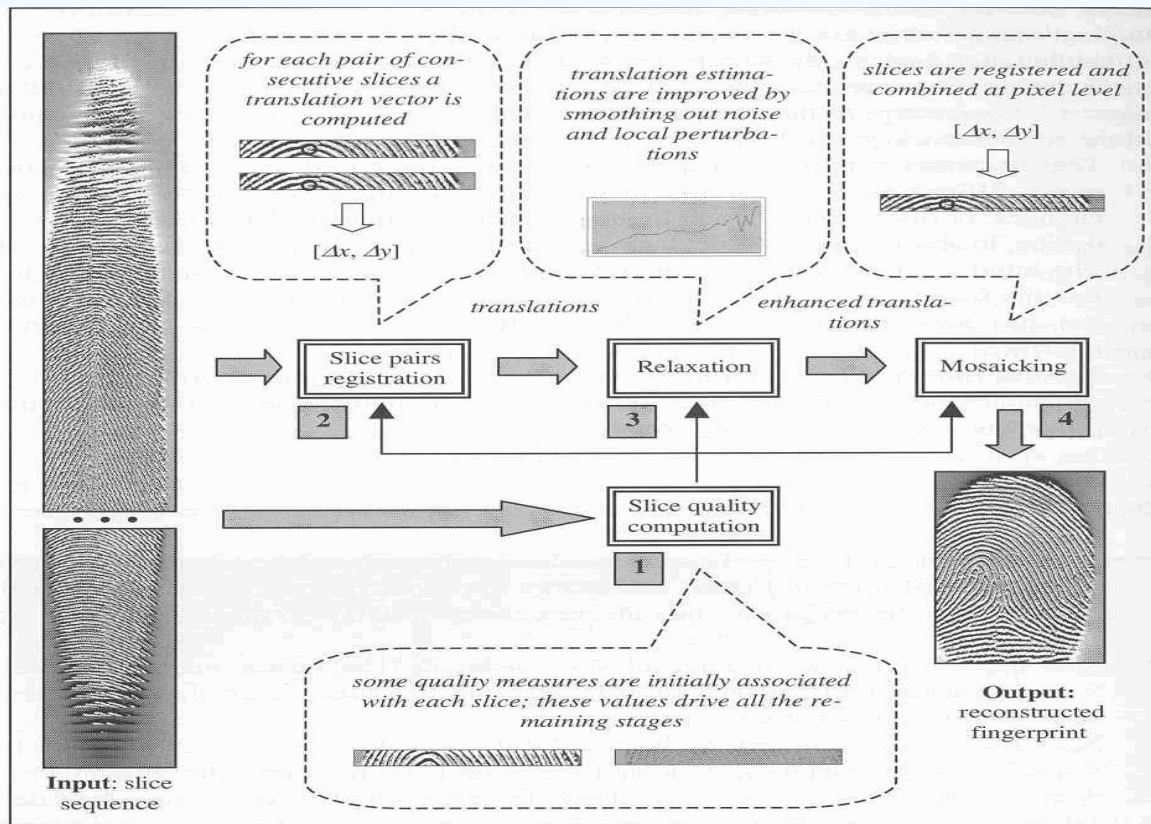


Figure 2.12. As the user sweeps her finger on the sensor, the sensor delivers new image slices, which are combined into a two-dimensional image.





Algorithm for fingerprint recognition from the slices



- Main stages are
- Slice quality computation
- Slice pair registration
- Relaxation
- Mosaicking

Figure 2.13. An algorithm for fingerprint reconstruction from slices. All the steps are performed sequentially on the whole set of slices. The output of the slice pair registration is a set of translation estimates that are globally enhanced by the relaxation step. These improved estimates drive the mosaicking phase in order to reconstruct the whole fingerprint image.





Figure 2.14. Fingerprint images of the same finger with ideal skin condition as acquired by different commercial scanners. Images are reported with right proportions: a) Biometrika FX2000, b) Digital Persona UareU2000, c) Identix DFR200, d) Ethentica TactilSense T-FPM, e) ST-Microelectronics TouchChip TCS1AD, f) Veridicom FPS110, g) Atmel FingerChip AT77C101B, h) Authentec AES4000.





Figure 2.15. Fingerprint images of the same dry finger as acquired by different commercial scanners. Images are reported with right proportions: a) Biometrika FX2000, b) Digital Persona UareU2000, c) Identix DFR200, d) Ethenica TactilSense T-FPM, e) ST-Microelectronics TouchChip TCS1AD, f) Veridicom FPS110, g) Atmel FingerChip AT77C101B, h) Authentec AES4000.





Figure 2.16. Fingerprint images of the same wet finger as acquired by different commercial scanners. Images are reported with right proportions: a) Biometrika FX2000, b) Digital Persona UareU2000, c) Identix DFR200, d) Ethentica TactilSense T-FPM, e) ST-Microelectronics TouchChip TCS1AD, f) Veridicom FPS110, g) Atmel FingerChip AT77C101B, h) Authentec AES4000.



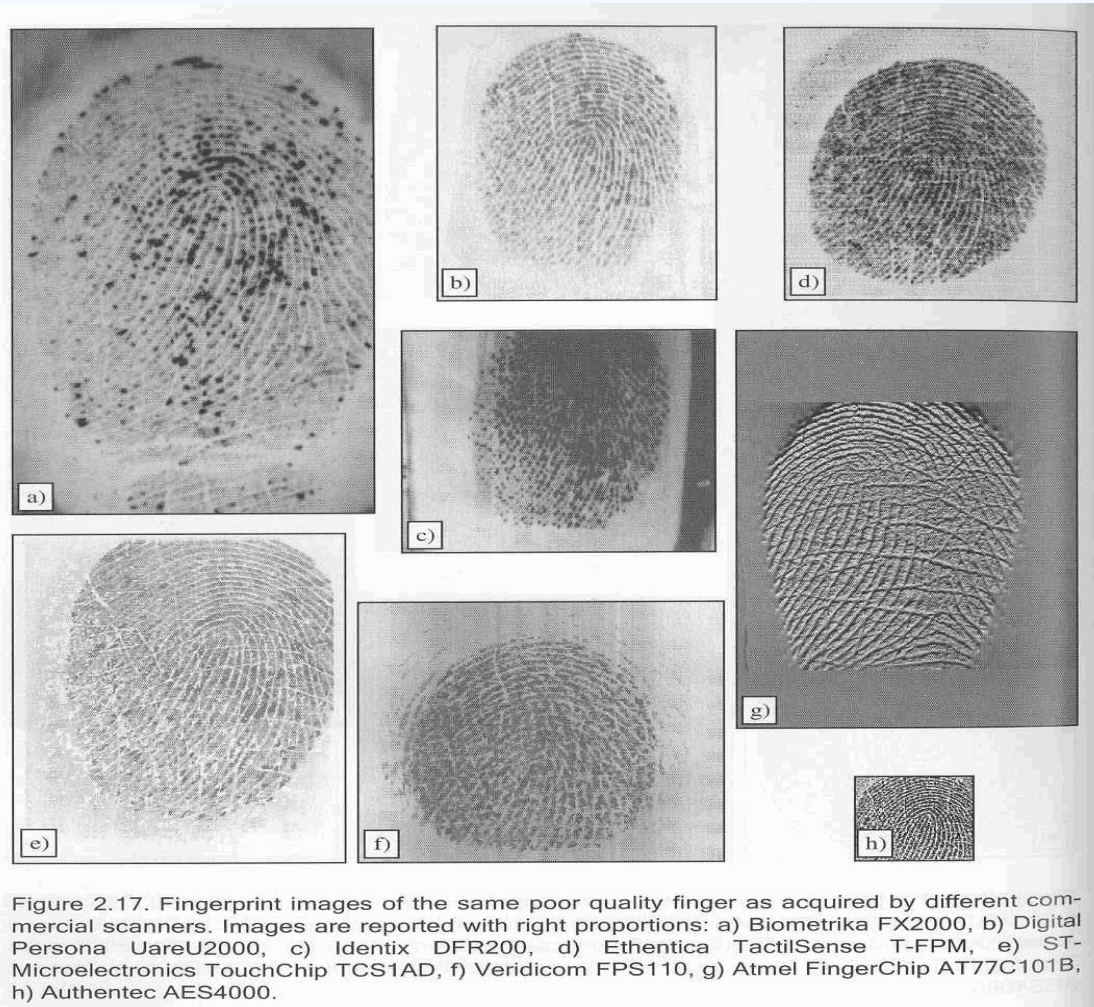


Figure 2.17. Fingerprint images of the same poor quality finger as acquired by different commercial scanners. Images are reported with right proportions: a) Biometrika FX2000, b) Digital Persona UareU2000, c) Identix DFR200, d) Ethenica TactilSense T-FPM, e) ST-Microelectronics TouchChip TCS1AD, f) Veridicom FPS110, g) Atmel FingerChip AT77C101B, h) Authentec AES4000.



Storing and Compressing fingerprint images



- Each fingerprint impression produces an image of 768 x 768 (when digitized at 500 dpi)
- In AFIS applications, this needs more amount of memory space to store these images
- Neither lossless methods or JPEG compression techniques are satisfactory
- A new compression technique called Wavelet Scalar Quantization (WSQ) is introduced to compress the images



DEMO, wavemenu



Wavelet 2-D -- Compression
1_1.jpg (374 x 388) analyzed at level 3 with db3

Original image Retained energy 97.76 % -- Zeros 97.76 %
Compressed image

Global threshold: 343.7
Retained energy: 97.76 %
Number of zeros: 97.76 %

Legend:
--- Global threshold
--- Retained energy in %
--- Number of zeros in %

Operations on selected image:
Visualize
Full Size
Reconstruct

Colormap: pink, Nb. Colors: 256, Brightness: +

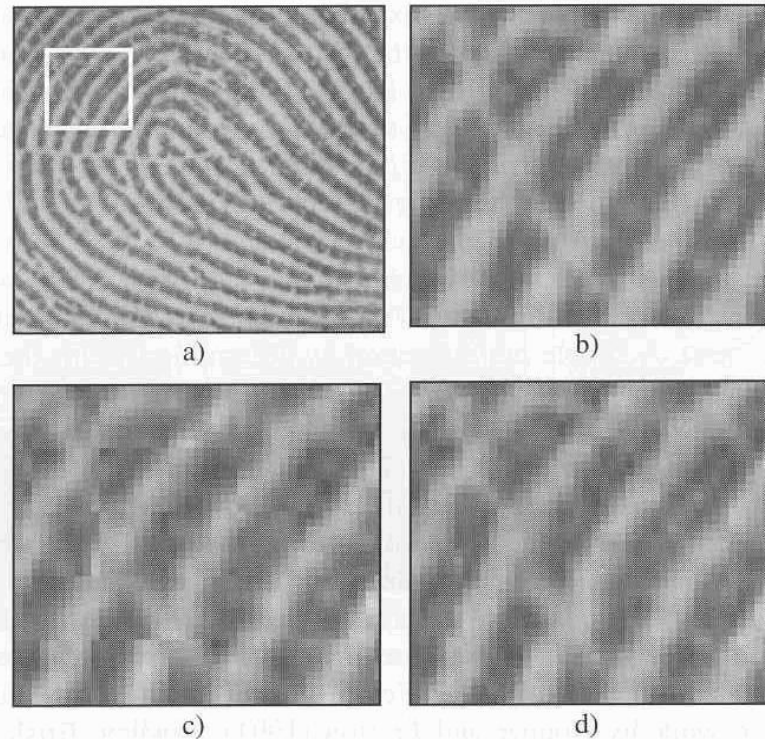


Figure 2.21. Fingerprint compression: a) the central section of a fingerprint image scanned at 500 dpi resolution; b) the marked portion of the image in a); c) the marked portion of the image in a) after the image was compressed using a generic JPEG (www.jpeg.org) image compression algorithm; and d) the marked portion of the image in a) is shown after the image was compressed using the WSQ compression algorithm. Both JPEG and WSQ examples used a compression ratio of 1:12.9; JPEG typically introduces blocky artifacts and obliterates detailed information. Images courtesy of Chris Brislawn, Los Alamos National Laboratory.





Enhancement, and Minutias Detection I

Daniel Novák

3.10.2019, Prague

**Acknowledgments: Xavier Palathingal, Andrzej Drygajlo,
Handbook of Fingerprint Recognition**



laboratory
Gerstner



Fingerprint

Interleaved ridges
and valleys

Ridge width: $100\mu\text{m}$
 $300\mu\text{m}$

Ridge-valley cycle:
 $500\mu\text{m}$

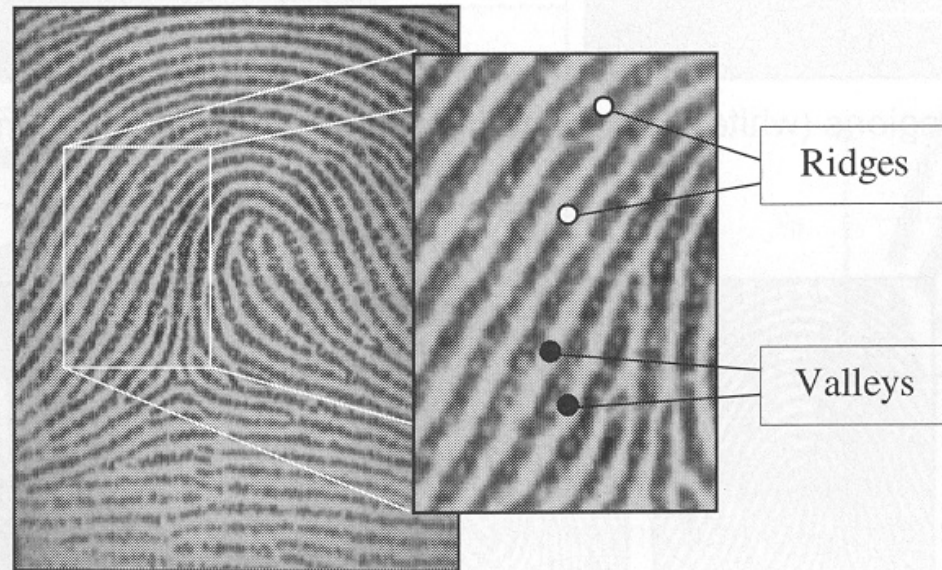


Figure 3.1. Ridges and valleys on a fingerprint image.



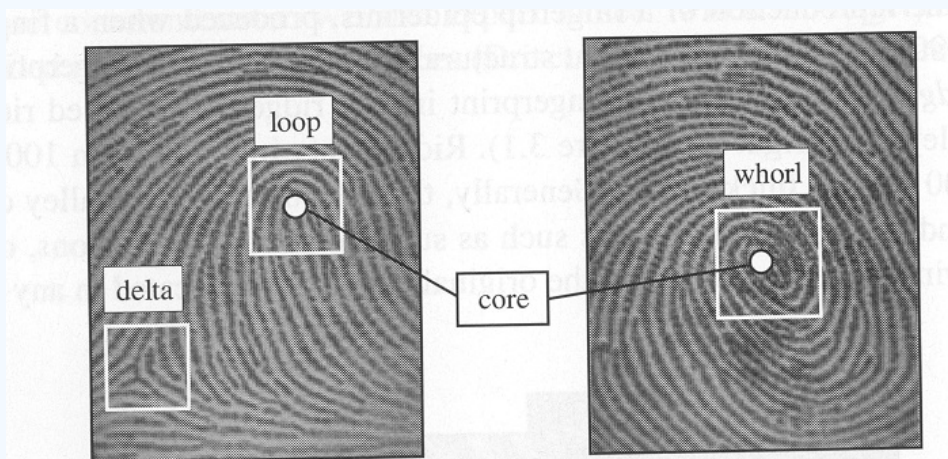
A Global Look

Singularities: In the global level the fingerprint pattern shows some distinct shapes

- Loop ()
- Delta (Δ)
- Whorl (O)...Two facing loop

Core:

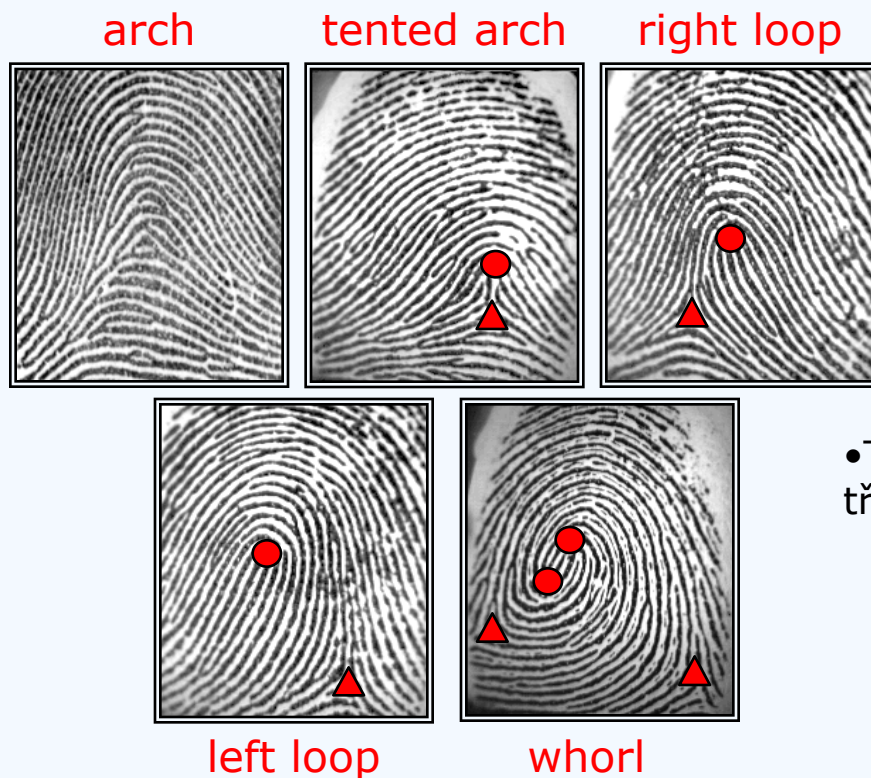
- A reference point for the alignment.
- The northmost loop type singularity.
- According to Henry(1900), it is the northmost point of the innermost ridgeline.
- Not all fingerprints have a core (Arch type fingerprints)





A Global Look

Singular regions are commonly used for fingerprint classification:



• Tzv Henryho systém, rozděluje otisky do pěti tříd

- Závit (whorl)
- Levá a pravá smyčka (loop)
- Oblouk (arch)
- Špičatý oblouk (tented arch)





Local Look

Minutia: Small details. Discontinuities in the ridges. (Sir Francis Galton)

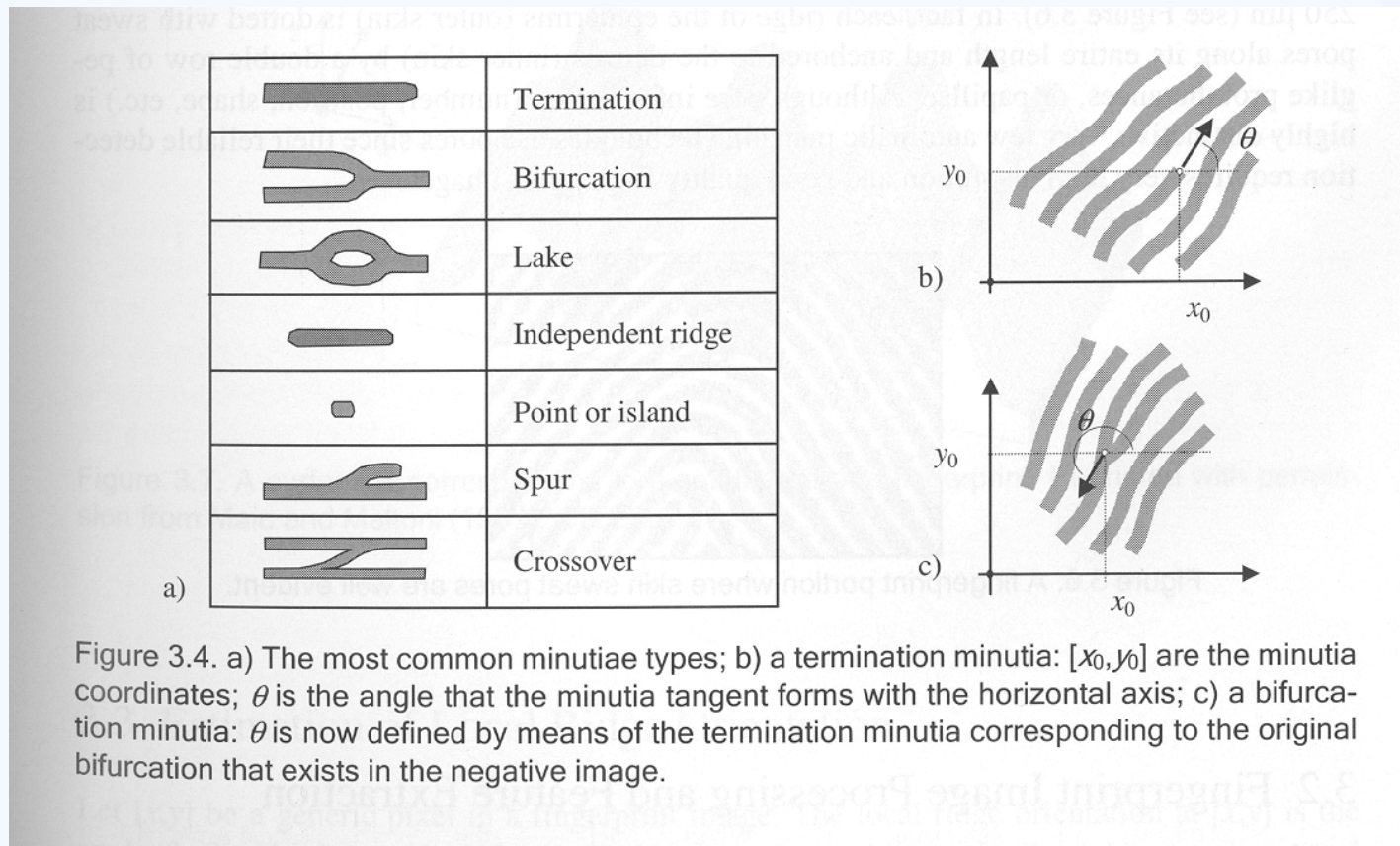


Figure 3.4. a) The most common minutiae types; b) a termination minutia: $[x_0, y_0]$ are the minutia coordinates; θ is the angle that the minutia tangent forms with the horizontal axis; c) a bifurcation minutia: θ is now defined by means of the termination minutia corresponding to the original bifurcation that exists in the negative image.



Terminologie



- Papilární linie
- Vyvýšeniny (ridge)+ prohlubeniny (furrow)
- Charakteristické body
 - Kritické (singulární) body – globálně význačné body
 - Jádro
 - Delta
 - Markanty (Minutiae) – lokálně význačné body
 - Rozvětvení (bifurcation)
 - Zakončení (ridge ending)
 - Krátké hrany (short ridge)
 - Překřížení (crossover, bridge)
 - Krátké rozvětvení (spur)
 - Očka (ridge enclosures)





Local Look

Ridge ending / ridge bifurcation **duality**

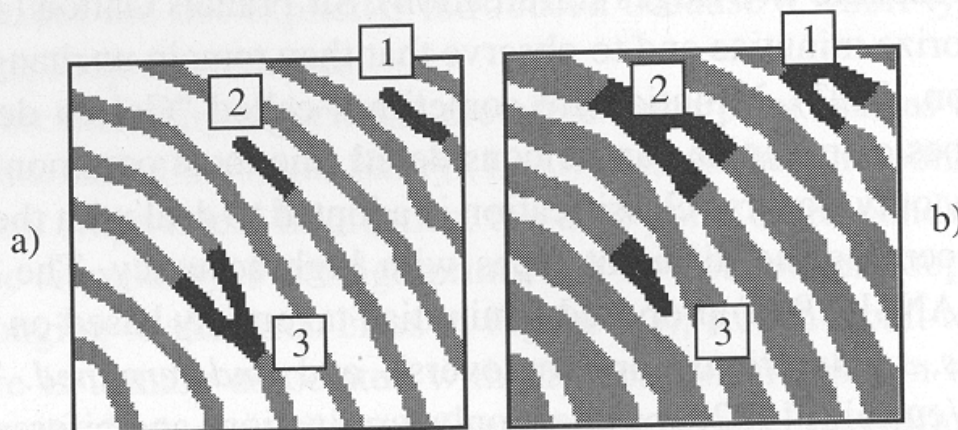


Figure 3.5. The termination/bifurcation duality on a) a binary image and b) its negative image.



Local Look

Sweat Pores

- High resolution images (1000 dpi)
- Size 60-250 μm
- Highly distinctive
- Not practical (High resolution, good quality images)



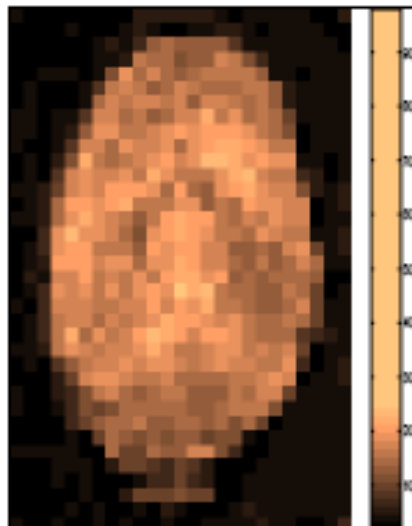
Figure 3.6. A fingerprint portion where skin sweat pores are well evident.



Segmentation



Original



Variance image



Segmented image

Segmentation is the process of isolating foreground from background:

- Image block (16x16 pixels) decomposition
- Thresholding using variance of gradient for each block

Segmentation



- Separating FP from background
- Straited patterns: no thresholding, striped and oriented pattern & isotropic pattern without orientation
- **Segmentation Methods (16x16 block)**
 - Variance orthogonal to the ridge direction [Ratha95]
 - Assumption: fingerprint area will exhibit high variance, where as the background and noisy regions will exhibit low variance.
 - Variance can also be used as the quality parameter of the regions.
 - High variance (high contrast): good quality
 - Low variance (low contrast): poor quality
 - Average magnitude of gradient in blocks
 - **Fp1 = segmentimage(Fp1);**





Enhancement, and Minutias Detection II

Daniel Novák

10.11, 2015, Prague

**Acknowledgments: Xavier Palathingal, Andrzej Drygajlo,
Handbook of Fingerprint Recognition**



laboratory
Gerstner

Estimation of Local Ridge Orientation



- Average orientation around indices i, j
- Unoriented directions
- Weighted (r_{ij})
- Gradient, maximum pixel-intensity change, $\arctan gy/gx$

$$\nabla f = \left(\frac{\partial f}{\partial x_1}, \dots, \frac{\partial f}{\partial x_n} \right).$$

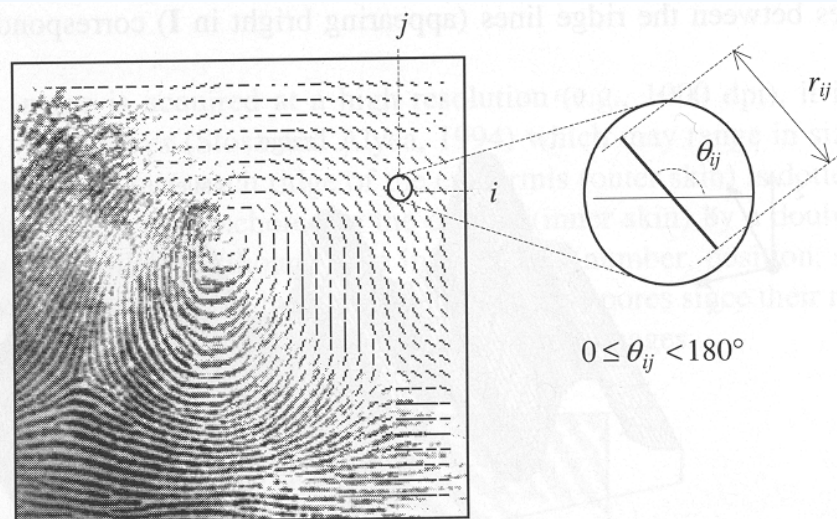


Figure 3.8. A fingerprint image faded into the corresponding orientation image computed over a square-meshed grid of size 16×16 . Each element denotes the local orientation of the fingerprint ridges; the element length is proportional to its reliability.



Estimation of Local Ridge Orientation



– Simple Approach

- Gradient with Sobel or Prewitt operators
- Θ_{ij} is orthogonal to the direction of the gradient

$$M_x = \begin{bmatrix} -1 & 0 & 1 \\ -1 & 0 & 1 \\ -1 & 0 & 1 \end{bmatrix} \quad M_y = \begin{bmatrix} -1 & -1 & -1 \\ 0 & 0 & 0 \\ 1 & 1 & 1 \end{bmatrix}$$

$$M_x = \begin{bmatrix} -1 & 0 & 1 \\ -2 & 0 & 2 \\ -1 & 0 & 1 \end{bmatrix} \quad M_y = \begin{bmatrix} -1 & -2 & -1 \\ 0 & 0 & 0 \\ 1 & 2 & 1 \end{bmatrix}$$

Drawbacks:

Non-linear and discontinuous around 90

A single estimate is sensitive to noise

Circularity of angles: Averaging is not possible

Averaging is not well defined.



Estimation of Local Ridge Orientation



–Averaging Gradient Estimates

(Kass, Witkin 1987)

$$d_{ij} = [r_{ij} \cdot \cos 2\theta_{ij}, r_{ij} \sin 2\theta_{ij}]$$

$$\bar{\mathbf{d}} = \left[\frac{1}{n^2} \sum_{i,j} r_{ij} \cdot \cos 2\theta_{ij}, \frac{1}{n^2} \sum_{i,j} r_{ij} \cdot \sin 2\theta_{ij} \right]$$

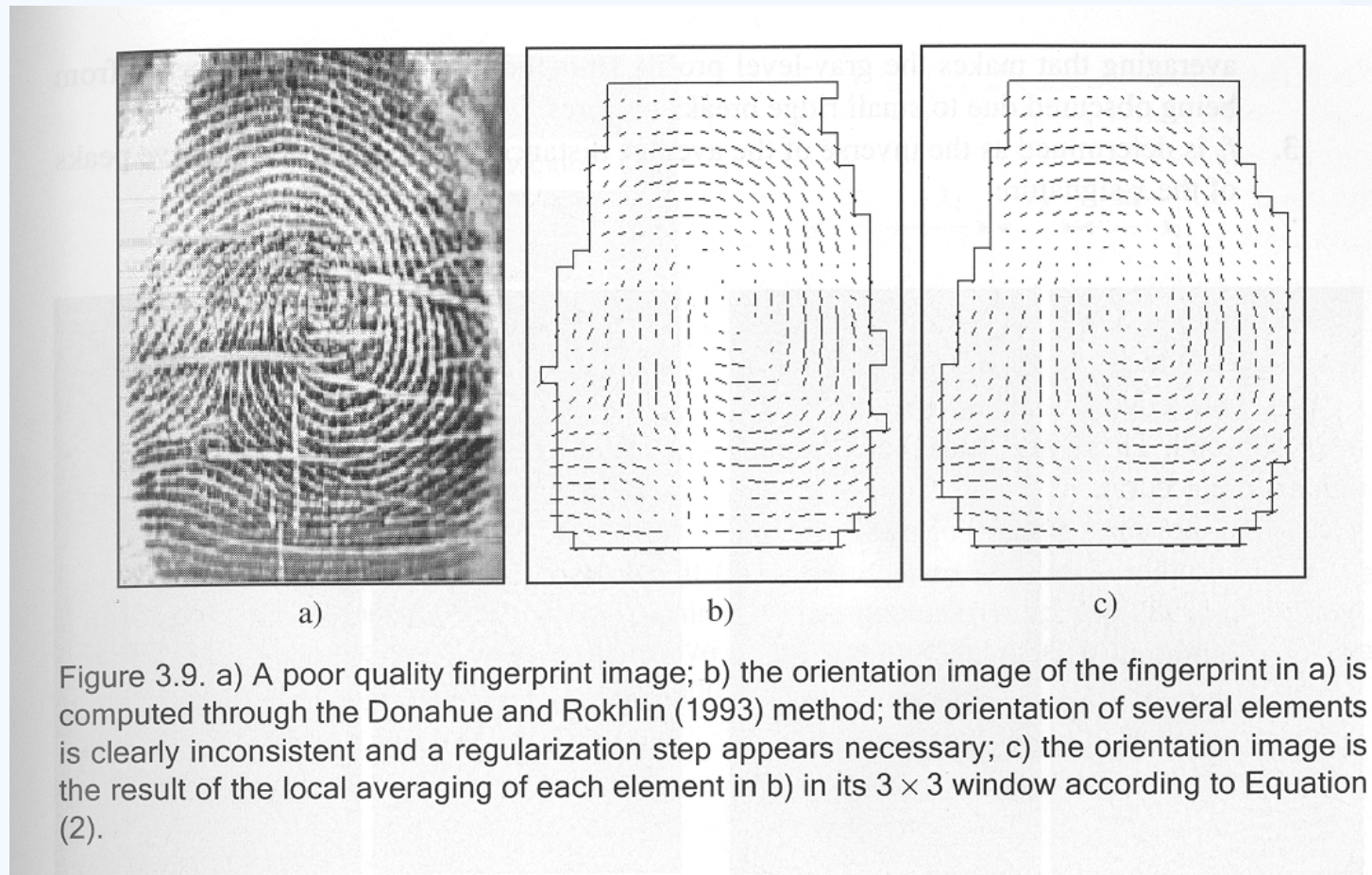
(2)

$$r = \nabla_x^2 + \nabla_y^2$$



Estimation of Local Ridge Orientation

– Effect of averaging



Orientation field



An orientation is calculated for each 16x16 block

- Compute the gradient of the smoothed block. $G_x(i,j)$ and $G_y(i,j)$ using 3x3 Sobel Masks
- Obtain the dominant direction in the block using the following equation:

$$\theta_d = \frac{1}{2} \tan^{-1} \left(\frac{\sum_{i=1}^{16} \sum_{j=1}^{16} 2G_x(i,j)G_y(i,j)}{\sum_{i=1}^{16} \sum_{j=1}^{16} (G_x(i,j)^2 - G_y(i,j)^2)} \right), G_x \neq 0 \text{ and } G_y \neq 0 \quad (1)$$

$$G_{xy} = \sum_{h=-8}^8 \sum_{k=-8}^8 \nabla_x(x_i+h, y_j+k) \cdot \nabla_y(x_i+h, y_j+k),$$

$$G_{xx} = \sum_{h=-8}^8 \sum_{k=-8}^8 \nabla_x(x_i+h, y_j+k)^2,$$

$$G_{yy} = \sum_{h=-8}^8 \sum_{k=-8}^8 \nabla_y(x_i+h, y_j+k)^2,$$

$$\theta_{ij} = 90^\circ + \frac{1}{2} \operatorname{atan} 2(2G_{xy}, G_{xx} - G_{yy})$$



- **DEMO: Fp1 = computeorientationarray(Fp1);**
- Gradient is computed by (standard): $[fx, fy] = \text{gradient}(\text{double}(\text{im}));$
- Block 10x10

Example: Orientation field

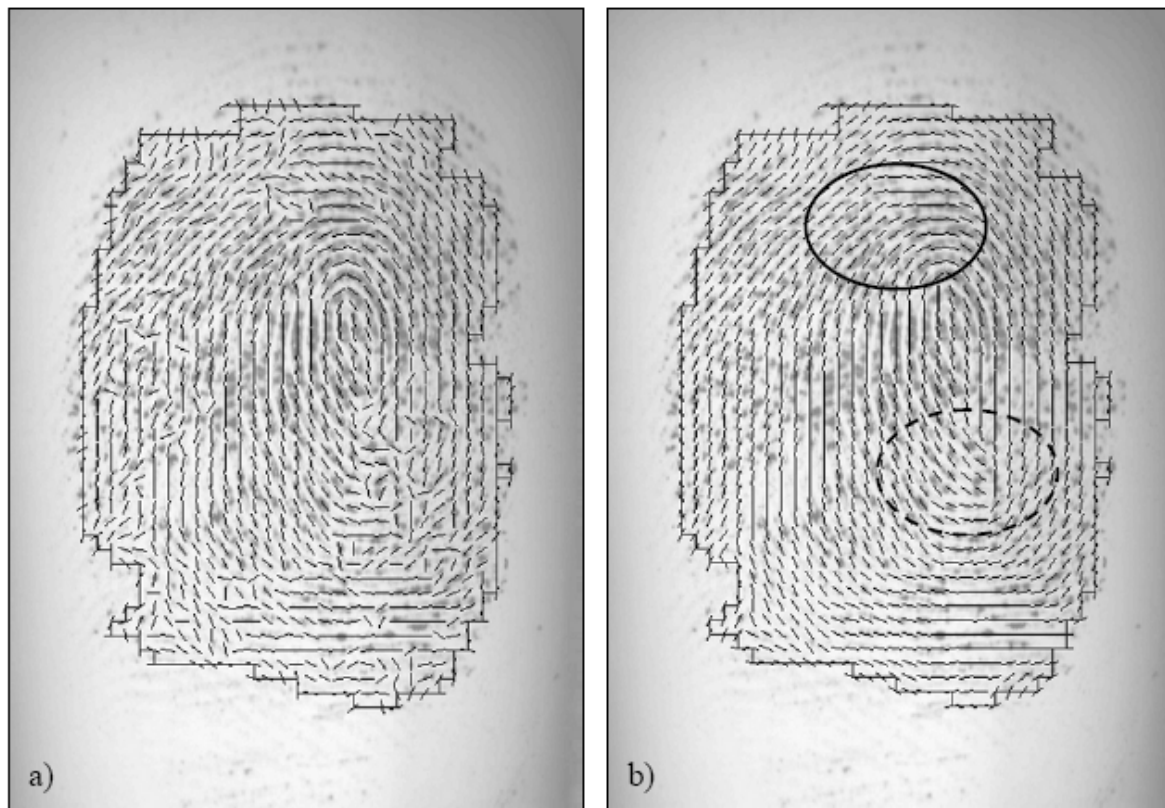
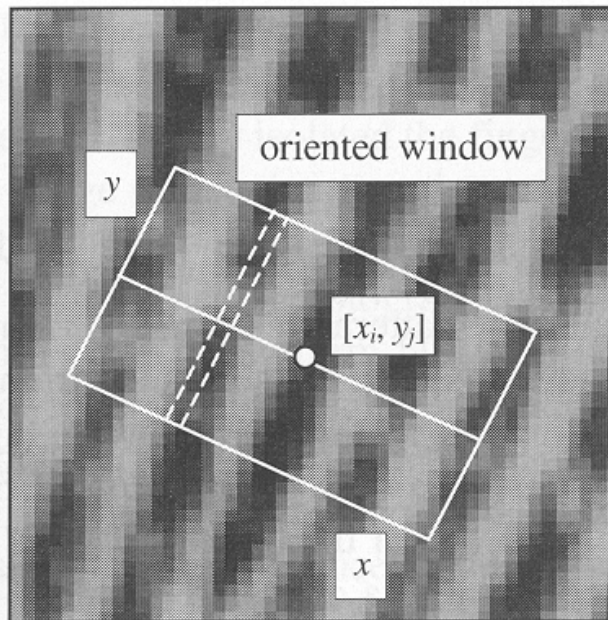


Figure 3.12. a) Estimation of local ridge orientation in a fingerprint through the gradient-based approach corresponding to Equation (3): in the noisy regions the estimation is unreliable; b) two iterations of local (3x3) smoothing are applied, resulting in a more consistent representation; it is worth noting that while the smoothing recovered the correct orientation at several places (e.g., inside the solid circle), it altered the average orientation inside the region denoted by the dashed circle where incorrect orientations were dominating the correct one.



Estimation of Local Ridge Frequency



$$f_{ij} = \frac{4}{s_1 + s_2 + s_3 + s_4}$$

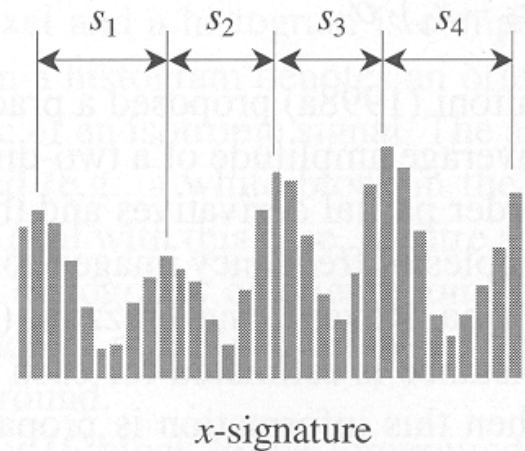


Figure 3.11. An oriented window centered at $[x_i, y_j]$; the dashed lines show the pixels whose gray-levels are accumulated for a given column of the x -signature (Hong, Wan, and Jain, 1998). The x -signature on the right clearly exhibits five peaks; the four distances between consecutive peaks are averaged to determine the local ridge frequency.

Estimation of Local Ridge Frequency



Simple Algorithm

- 1) 32x16 oriented window centered at $[x_i, y_i]$
- 2) The x-signature of the grey levels is obtained
- 3) f_{ij} is the inverse of the average distance

To handle noise interpolation and/or low pass filtering is applied.



DEMO: `Fp1 = computelocalfrequency(Fp1, Fp1.imOriginal);`

Estimation of Local Ridge Frequency



– Examples of frequency maps

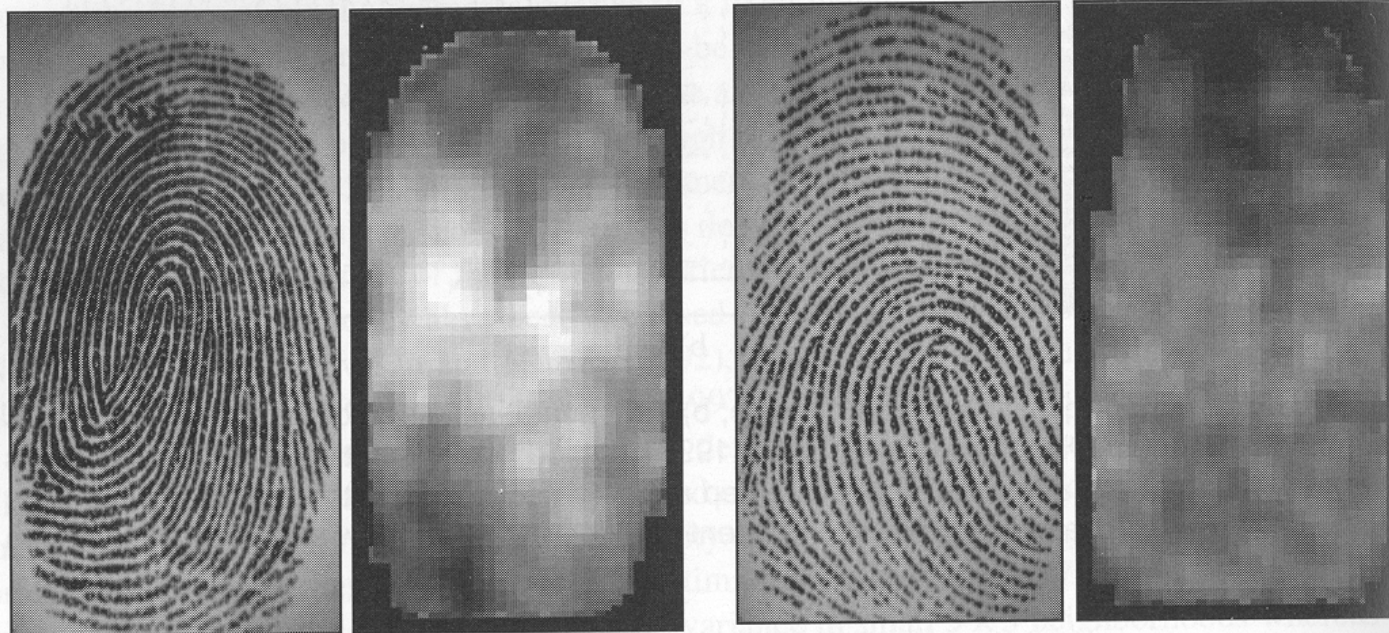


Figure 3.10. Two fingerprint images and the corresponding frequency image computed with the method proposed by Maio and Maltoni (1998a). A local 3×3 averaging is performed after frequency estimation to reduce noise. Light blocks denote higher frequencies. It is quite evident that significant changes may characterize different fingerprint regions and different average frequencies may result from different fingers.



Contextual Filters



- The most widely used technique for fingerprint image enhancement
- Conventional image filtering – a single filter is used for convolution throughout
- Contextual filtering - filter characteristics change according to local context
- Several types of contextual filters proposed
- Indented behavior –
 - 1) provide a low-pass [averaging] effect along the ridge direction.
Linking small gaps and filling impurities due to noise
 - 2) perform a band pass [differentiating] in the direction orthogonal to the ridges
Increase discrimination between ridges and valleys



Method proposed by Hong, Wan, and Jain



- Based on Gabor filters
- Gabor filters have both frequency-selective and orientation-selective properties and have optimal joint resolution in spatial and frequency domains
- A Gabor filter is defined by a sinusoidal plane wave tapered by a Gaussian

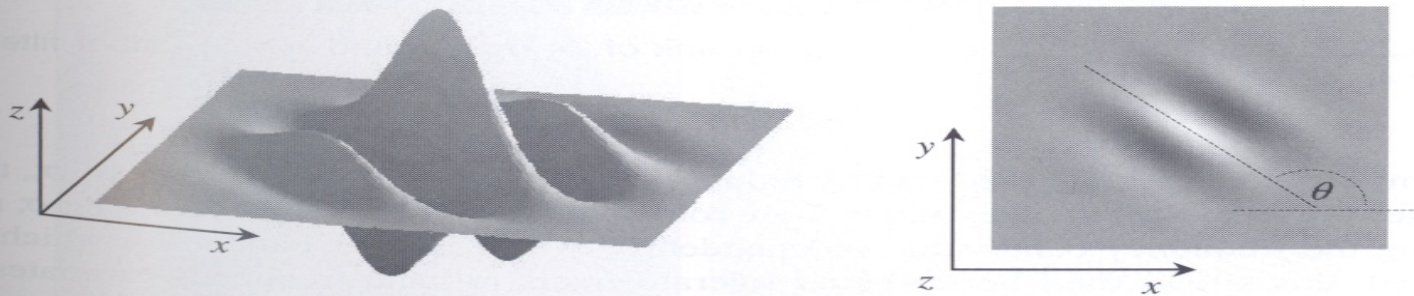


Figure 3.28. Graphical representation (lateral view and top view) of the Gabor filter defined by the parameters $\theta = 135^\circ$, $f = 1/5$, and $\sigma_x = \sigma_y = 3$.

Method proposed by Hong, Wan, and Jain (cont ..)



The even symmetric two-dimensional Gabor filter has the following form:

$$g(x, y; \theta, f) = \exp\left\{-\frac{1}{2}\left[\frac{x_\theta^2}{\sigma_x^2} + \frac{y_\theta^2}{\sigma_y^2}\right]\right\} \cdot \cos(2\pi f \cdot x_\theta), \quad (5)$$

where θ is the orientation of the filter, and $[x_\theta, y_\theta]$ are the coordinates of $[x, y]$ after a clockwise rotation of the Cartesian axes by an angle of $(90^\circ - \theta)$.

$$\begin{bmatrix} x_\theta \\ y_\theta \end{bmatrix} = \begin{bmatrix} \cos(90^\circ - \theta) & \sin(90^\circ - \theta) \\ -\sin(90^\circ - \theta) & \cos(90^\circ - \theta) \end{bmatrix} \begin{bmatrix} x \\ y \end{bmatrix} = \begin{bmatrix} \sin\theta & \cos\theta \\ -\cos\theta & \sin\theta \end{bmatrix} \begin{bmatrix} x \\ y \end{bmatrix}.$$

Here, f is the frequency of a sinusoidal plane wave and σ_x and σ_y are the standard deviations of the Gaussian envelope along the x and y axes



Method proposed by Hong, Wan, and Jain (cont ..)

Gabor Filter



- 4 parameters – $\theta, f, \sigma_x, \sigma_y$
- The selection of the values σ_x and σ_y involves a tradeoff
- A set $\{g_{ij}(x,y) \mid i=1\dots n_0, 1\dots n_f\}$ of filters are priori created and stored, where n_0 is the number of discrete orientations $\{\theta_i \mid i=1, \dots, n_0\}$ and n_f the number of discrete frequencies $\{f_j \mid j=1, \dots, n_f\}$
- Each pixel $[x,y]$ is convolved, with filter $g_{ij}(x,y)$ such that θ_i is the discretized orientation closest to θ_{xy} and f_j is the discretized orientation closest to f_{xy}
- **DEMO: Fp1 = enhance2ridgevalley(Fp1);**

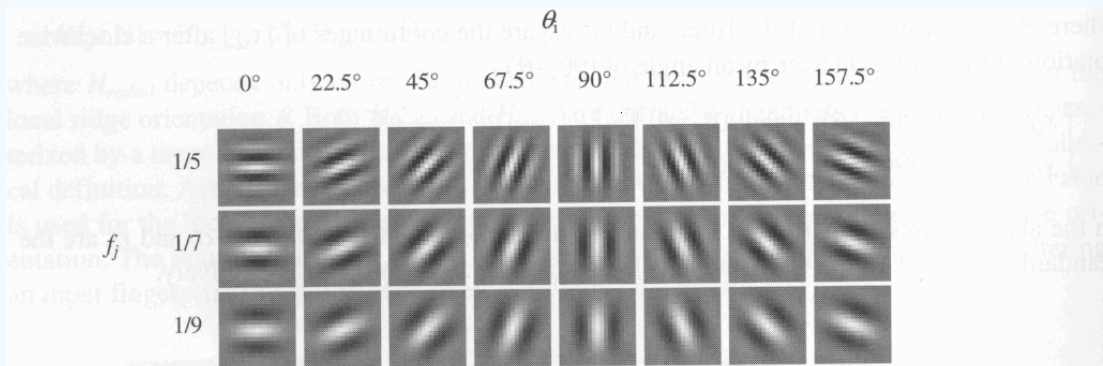


Figure 3.29. A graphical representation of a bank of 24 ($n_0 = 8$ and $n_f = 3$) Gabor filters where $\sigma_x = \sigma_y = 4$.



Method proposed by Hong, Wan, and Jain (cont ..)

– Examples



- Shows the application of Gabor-based contextual filtering on medium and poor quality images

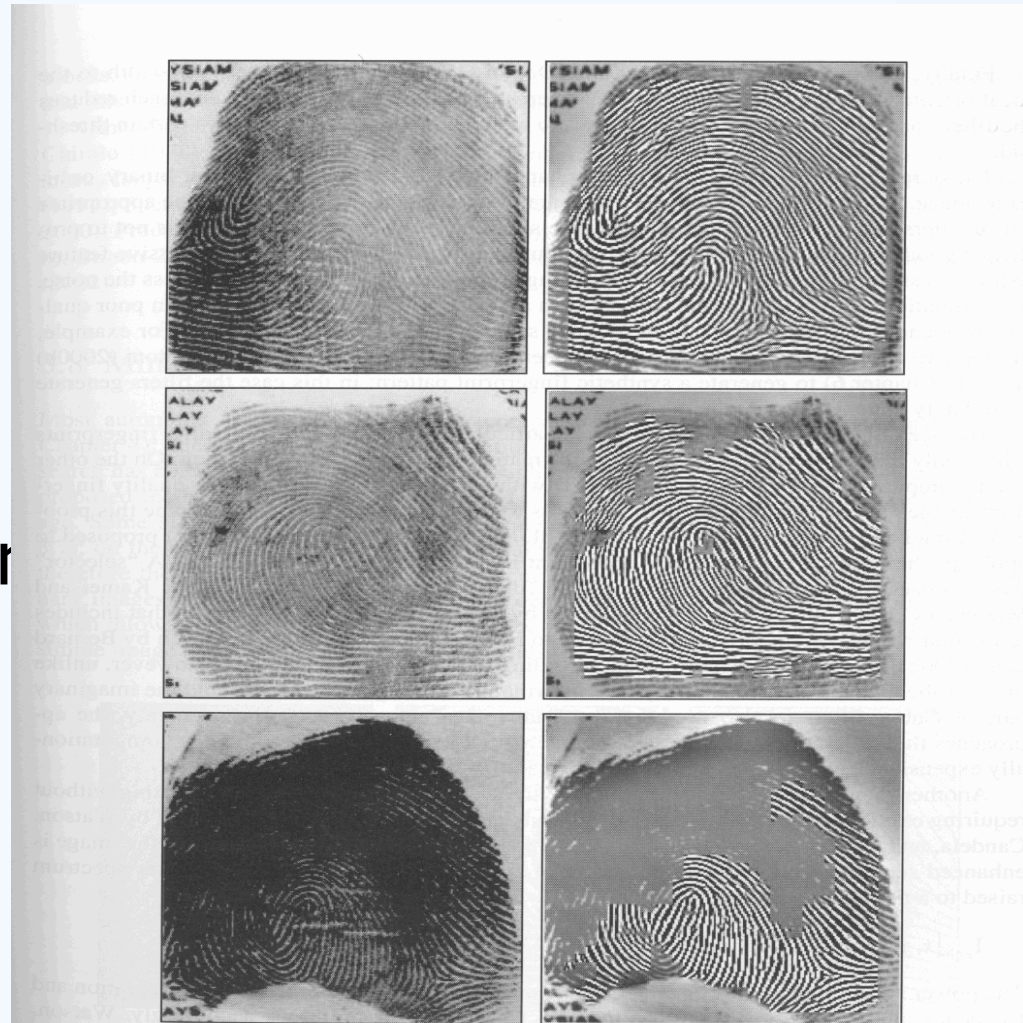


Figure 3.30. Examples of fingerprint enhancement with Gabor filtering as proposed by Hong, Wan, and Jain (1998). On the right, the enhanced recoverable regions are superimposed on the corresponding input images. ©IEEE.



Minutiae Detection



- Reliable minutiae extraction is extremely important
 - Binarization
 - Thinning
 - Post processing – filling holes, linking breaks, removing bridges

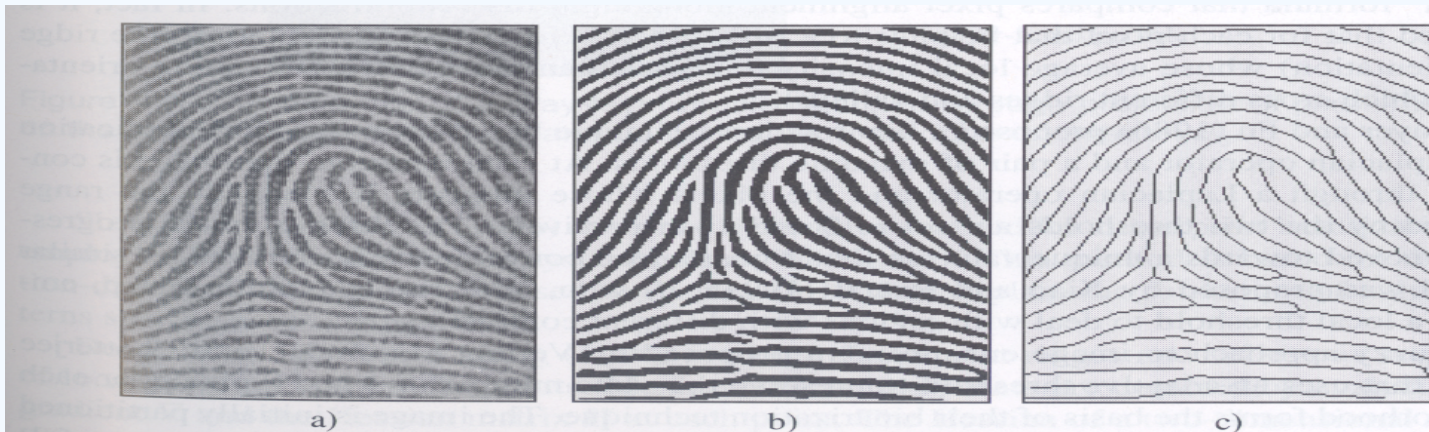


Figure 3.31. a) A fingerprint gray-scale image; b) the image obtained after a binarization of the image in a); c) the image obtained after a thinning of the image in b). Reprinted with permission from Maio and Maltoni (1997). ©IEEE.



Binarization-based methods



- Simplest method - global threshold
- Local threshold technique
- Fingerprint specific solutions necessary

**Binarization is the output of Contextual Filtering:
enhance2ridgevalley.m**

```
binaryBlkSize = 20;
```

```
imReconstruct = blkproc(imReconstruct, [binaryBlkSize  
    binaryBlkSize], @binarizeimage);
```

```
function Iout = binarizeimage(Iin)
```

```
level = graythresh(Iin); %Otsu method
```

```
Iout = im2bw(Iin, level);
```



Threshold computation: Otsu I



- Otsu's method: *N. Otsu (1979). "A threshold selection method from gray-level histograms". IEEE Trans. Sys., Man., Cyber. 9: 62–66*
 - http://en.wikipedia.org/wiki/Otsu%27s_method
 - http://homepages.inf.ed.ac.uk/rbf/CVonline/LOCAL_COPIES/MORSE/threshold.pdf
- minimizes the intra-class variance – for each threshold T lot's of work

$$\sigma_{\text{Within}}^2(T) = n_B(T)\sigma_B^2(T) + n_O(T)\sigma_O^2(T)$$

- between-class variance:

$$\begin{aligned}\sigma_{\text{Between}}^2(T) &= \sigma^2 - \sigma_{\text{Within}}^2(T) \\ &= n_B(T) [\mu_B(T) - \mu]^2 + n_O(T) [\mu_O(T) - \mu]^2\end{aligned}$$

$$n_B(T) = \sum_{i=0}^{T-1} p(i)$$

$$n_O(T) = \sum_{i=T}^{N-1} p(i)$$

$\sigma_B^2(T)$ = the variance of the pixels in the background (below threshold)

$\sigma_O^2(T)$ = the variance of the pixels in the foreground (above threshold)

where σ^2 is the combined variance and μ is the combined mean

Threshold computation: Otsu II



- Compute histogram and probabilities of each intensity level
- Set up initial $n_b(0)$ and $n_o(0)$ and $\mu_b(0)$, $\mu_o(0)$
- Step through all possible thresholds $T=1 \dots$ maximum intensity
 - Update $n_b(T), n_o(T)$
 - Compute $\sigma_{\text{between}}(T)$
- Desired threshold corresponds to the maximum $\sigma_{\text{between}}(T)$



Minutiae detection

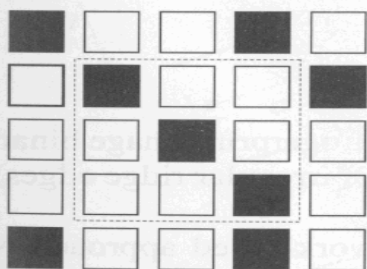


- A simple image scan allows the pixel corresponding to minutiae to be detected
- *crossing number* of a pixel p
- **DEMO: Fp1 = cleanskeleton(Fp1);**

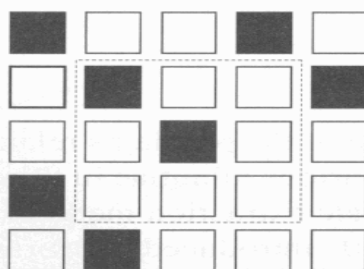
$$cn(\mathbf{p}) = \frac{1}{2} \sum_{i=1..8} |val(\mathbf{p}_{i \bmod 8}) - val(\mathbf{p}_{i-1})|,$$

where $\mathbf{p}_0, \mathbf{p}_1, \dots, \mathbf{p}_7$ are the pixels belonging to an ordered sequence of pixels defining the 8-neighborhood of \mathbf{p} and $val(\mathbf{p}) \in \{0,1\}$ is the pixel value. It is simple to note (Figure 3.36) that a pixel \mathbf{p} with $val(\mathbf{p}) = 1$:

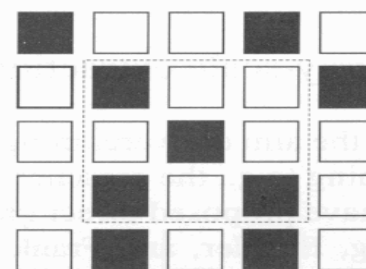
- is an intermediate ridge point if $cn(\mathbf{p}) = 2$;
- corresponds to a termination minutia if $cn(\mathbf{p}) = 1$;
- defines a more complex minutia (bifurcation, crossover, etc.) if $cn(\mathbf{p}) \geq 3$.



a) $cn(\mathbf{p}) = 2$



b) $cn(\mathbf{p}) = 1$



c) $cn(\mathbf{p}) = 3$

Figure 3.36. a) intra-ridge pixel; b) termination minutia; c) bifurcation minutia.



Examples of minutiae extraction

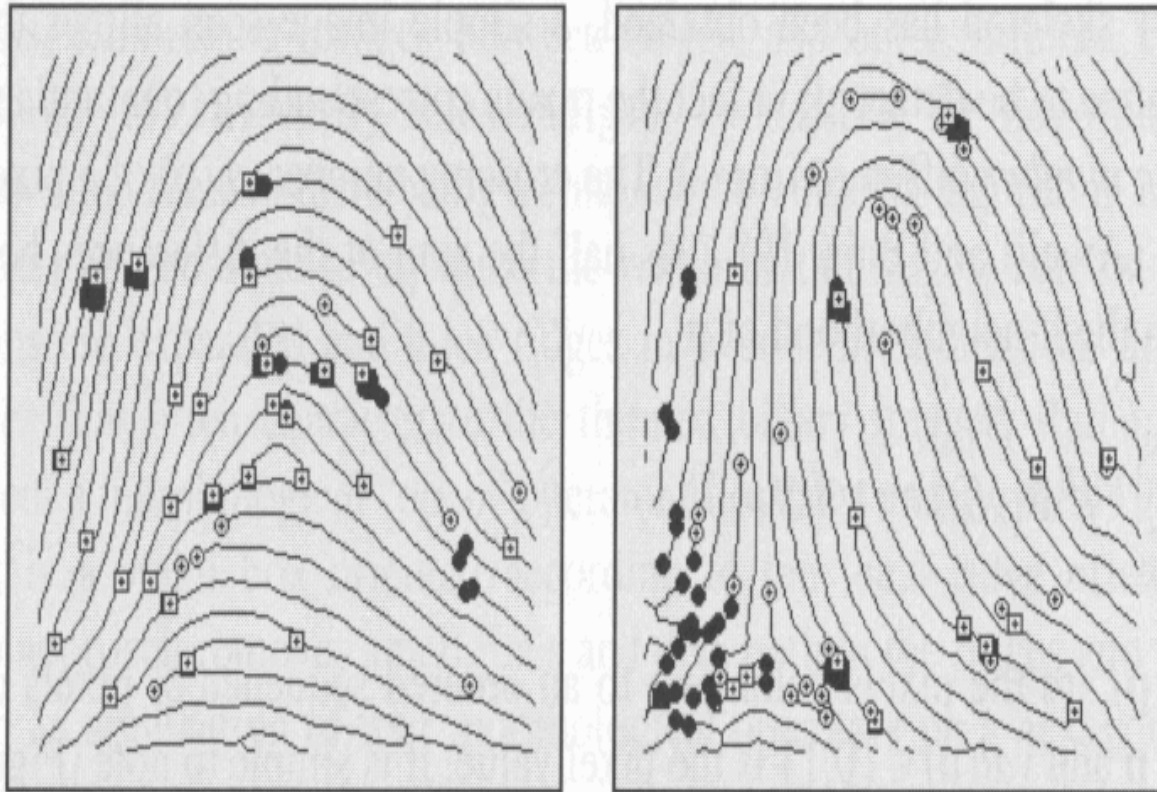
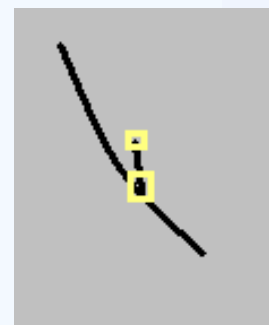
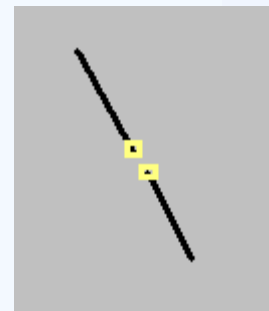


Figure 3.37. Examples of minutiae detection on binary skeletons. White circles and white boxes denote terminations and bifurcations, respectively; black circles and black boxes denote filtered minutiae (see Section 3.9).



Minutiae Filtering

- Post-processing stage is useful for removing spurious minutiae [already present or introduced by previous steps]
- Two main post-processing types:
 - Structural post-processing
 - Minutiae filtering in the gray-scale domain
- Ridge breaks (insufficient ink or moist)
- Ridge cross-connections (over-ink, over-moist)
- Boundaries



Example

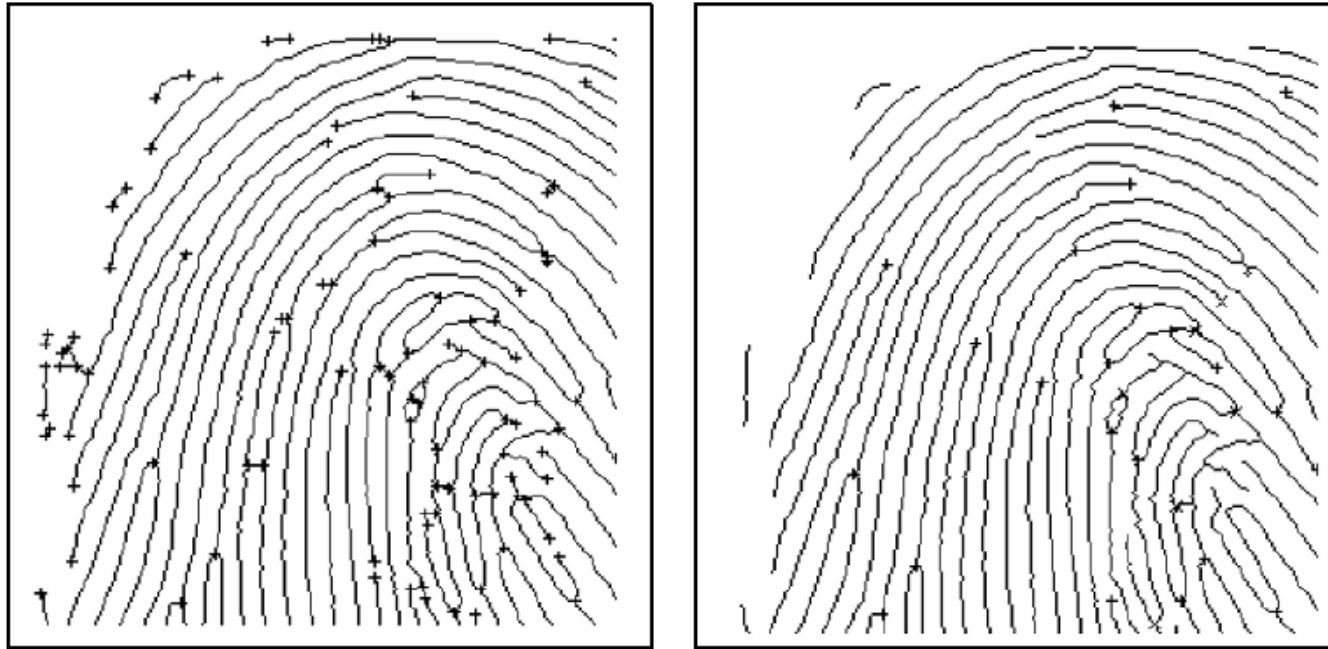


Figure 3.51. Minutiae post-processing according to Farina, Kovacs-Vajna, and Leone (1999). On the right, most of the false minutiae present in the thinned binary image (on the left) have been removed. © Elsevier.